Drinking water biofiltration: behaviour of antibiotic resistance genes and the association with bacterial community

Like Xu, Luiza C. Campos, Melisa Canales, Lena Ciric *

Department of Civil, Environmental & Geomatic Engineering, University College London, London, WC1E 6BT, UK

* Corresponding author: Lena Ciric, l.ciric@ucl.ac.uk

Abstract

Antibiotic resistance genes (ARGs) are being detected in drinking water frequently, constituting a major public health issue. As a typical drinking water treatment process, the biofilter may harbour various ARGs due to the filter biofilms established during the filtration process. The objective of this study was to investigate the behaviour of ARGs (*bla*$_{CTX-M}$, *bla*$_{OXA-1}$, *bla*$_{TEM}$, *ermB, tetA, tetG, tetQ, tetW, tetX, sul 1, sul 2, dfrA1 and dfrA12*) and their possible association with bacteria in a bench-scale biofiltration system. The impact of filter media on horizontal gene transfer (HGT) was also explored using a model conjugative plasmid, RP1. The biofiltration system comprised four types of biofilters, including sand, granular activated carbon (GAC), GAC sandwich, and anthracite-sand biofilters. Results showed that although the absolute abundance of ARGs decreased (0.97-log reduction on average), the ARGs' abundance normalised to bacterial numbers showed an increasing trend in the filtered water. Biofilms collected from the surface layer revealed the lowest relative abundance of ARGs ($p < 0.01$) compared to the deeper layer biofilms, indicating that the proportion of ARG-carrying bacteria was greater in the lower position. Most chosen ARG numbers correlated to *Proteobacteria*, *Acidobacteria* and *Nitrospirae* phyla, which accounted for 51.9%, 5.2% and 2.0% of the biofilm communities, respectively. GAC media revealed the highest transfer frequency (2.60×10^{-5}), followed by anthracite (5.31×10^{-6}) and sand (2.47×10^{-6}). Backwashing can reduce the transferability of RP1 plasmid significantly in biofilms but introduces more transconjugants into the planktonic phase. Overall, the results of this study could enhance our understanding of the prevalence of ARGs in drinking water biofiltration treatment.

Keywords: Biofiltration; Antibiotic resistance genes; Biofilm; Bacterial community; Horizontal gene transfer

1. Introduction

Antibiotic resistance genes (ARGs) are diverse and ubiquitous in natural environments. Hundreds of ARGs were detected in various environmental matrices, including wastewater treatment plants, livestock, aquaculture, surface water, soil and sediment (Chen *et al*., 2016; Gao *et al*., 2012; Wang *et al*., 2014). The high mobility of microorganisms in the water phase has rendered the aquatic environment an important reservoir for ARGs (Zhang *et al*., 2009). ARGs remaining in source waters (e.g. river and lake water) have the potential to reach tap water via drinking water treatment plants (DWTPs) and distribution systems. For instance, the concentration of ARGs in source waters used for drinking water production ranged from 10^8 to 10^9 copies/L (Xu *et al*., 2016), which is comparable to ARGs levels (4.33×10^8 copies/L, mean value) in a large scale case study investigating 42 natural waterbodies across China (Liu *et al*., 2018). Moreover, enhanced levels of ARGs with an enrichment of up to 100-fold in tap water after pipeline transportation was observed in Xu *et al*.' study (2016), raising concerns from both researchers and the public.

Biofiltration is a simple and cost-effective drinking water treatment technology, which allows the microorganisms in the source water to attach and colonise the surface of granular media and develop a biofilm (Sharma et al., 2018). Filter media commonly used for biofiltration include sand, granular activated carbon (GAC) and anthracite. Due to the high bacterial density and diversity sustained, drinking water biofilms have shown to facilitate horizontal gene transfer (HGT) of ARGs under environmental conditions (Schlüter *et al*., 2007). For instance, *vanA* (a vancomycin resistance gene) has been detected in drinking water biofilms without the presence of bacterial host *enterococci*, indicating the potential transfer of *vanA* to indigenous drinking water bacteria (Schwartz *et al*., 2003). In addition, Farkas *et al.* (2003) reported that the biofilm community in a DWTP is a reservoir of class 1 integrons, indicating that the drinking water biofilm has the potential to accumulate resistance determinants. The above observations suggest that the biofilm may serve as an ideal site for ARG transfer in aquatic

environments. However, the mechanisms underlying the occurrence of HGT during biofiltration and the impact of filter media on HGT both remained unknown.

The understanding of microbial composition in the filter media is essential in the context of microbial risk as it could dictate the microbiological quality of the effluent and shape the bacterial community structure in the drinking water microbiome (de Vera *et al*., 2018; Pinto *et al*., 2012). Variation in antibiotic resistome during drinking water treatment processes is generally associated with the bacterial community. For instance, Jia *et al*. (2015) have found that sulfonamide resistance genes were carried by *Salmonella*, while most of aminoglycoside resistance genes were carried by *Pseudomonas* and *Escherichia* in drinking water; Zheng *et al.* (2018) reported that *Firmicutes* was mostly related to persistent ARGs in activated carbon biofilms collected from a DWTP. Moreover, they discovered that *Firmicutes* organisms were able to communicate with each other through quorum sensing in GAC biofilms with respect to selective pressure from the environment and accelerating the ARG transfer. A lab-scale biofiltration study suggested that the bacterial community composition in the sand biofilm is associated with the antibiotic resistome (Wan *et al*., 2019). In general, previous research has focused on a single medium used in biofiltration, comparisons among representative filter media and their correlations with ARG abundance during biofiltration are still unknown.

In this study, two sets of biofiltration columns were set-up at bench-scale. The first biofiltration system comprised of four types of biofilters, including sand, GAC, GAC sandwich, and anthracite-sand biofilters in order to explore the behaviour of ARGs during the filtration process and the possible relationship between ARGs and bacterial community structure in filter biofilms. Natural surface water spiked with sulfamethoxazole, trimethoprim, amoxicillin, oxytetracycline, and clarithromycin was used as feedwater for all biofilters. The selection of the target antibiotics was based on their presence in drinking water source waters. A total of 13 ARGs, including $bla_{CTX\text{-}M}$, $bla_{OXA\text{-}1}$, bla_{TEM}, *ermB, tetA, tetG, tetQ, tetW, tetX, sul 1, sul 2, dfrA1 and dfrA12* and integrase genes, *intI* 1 and *intI* 2 were selected in this study. The selection of ARGs was based on the antibiotic to which they confer resistance and their prevalence in surface waters. The second biofiltration experiment involved setting-up a

conjugative transfer system using the RP1 plasmid to explore the impact of filter media and antibiotic exposure on horizontal conjugative transfer. Overall, the results of this study could enhance our understanding of the prevalence of ARGs in drinking water biofiltration treatment.

2. Methods and materials

2.1 Biofiltration system setup and operation

Sand (SB), GAC (GB), GAC sandwich (GSB), and anthracite-sand (ASB) representing four types of biofilter were set-up in parallel at bench scale. Each biofilter type was run in duplicate. An overview of the biofilter systems setup and the composition of biofilters is shown in Figure 1. The biofiltration system consisted of eight columns, each with 36 cm of filter media (sand: effective size (ES) 0.20 mm, uniformity coefficient (UC) 1.82; GAC: ES 0.72 mm, UC 1.68; anthracite: ES 0.90 mm, UC 1.32) and 5 cm of support media (0.6–3 mm gravel). Surface characteristics of the filter media are shown in Figure S1. The feedwater for all biofilters was natural lake water collected from Regent's Park, London. A total of 25 L raw water was collected twice a week from October 2017 to January 2018. A dual head peristaltic pump (Watson-Marlow 323 U) with eight channels was introduced to simultaneously deliver feedwater to biofilters from the reservoir. Biofilter configurations are shown in Figure S2.

The biofilters were run under a hydraulic loading rate of 0.06 m/h, which was within the typical range of 0.04 to 0.4 m/h in use for slow sand filtration (D'Alessio *et al*., 2015; Letterman and Association, 1991). The biofiltration system was operated continuously for 11 weeks, including 4 weeks of biofilter maturation, when total coliforms and *Escherichia coli* achieved 2-log reduction (data not shown) (Huisman and Wood, 1974), and 7 weeks' exposure to antibiotics (2 µg/L of sulfamethoxazole, trimethoprim, oxytetracycline, and clarithromycin and 5 µg/L of amoxicillin) followed by a backwash/cleaning process at the end. Except for the GAC sandwich, biofilters were backwashed by pumping their own effluent upflow to achieve a 20 - 30% bed expansion (Liu *et al*., 2012). Each biofilter was backwashed for 10 min. The GAC sandwich was cleaned by stirring the top layer sand and the mixture of 'dirty' water was then withdrawn from above the filter at the same time (Reungoat *et al*., 2011). The system run continuously for 24 h after backwashing/cleaning was conducted.

2.2 Sample collection, DNA extraction and qPCR

Influent samples were taken immediately before entering the biofilters and mixed as one sample to capture an accurate influent concentration, while effluents were collected in drainage pipes located in the bottom of the biofilter and led by gravity to the outlets. A total of five batches of influent and effluent samples were collected throughout this study, including the week after the addition of antibiotics (batch 1) and then every two weeks thereafter (batch 2-4). Samples were also collected after the backwashing/cleaning of biofilters (batch 5). Sand, GAC and anthracite media samples at different depths of the filter bed were withdrawn from the sampling ports twice during the experimental period, *i.e.* at the end of the maturation stage (4 weeks) and before biofilter backwashing/cleaning (7 weeks), to collect the associated biofilm for genomic DNA extraction.

To separate bacterial cells from media particles, sand, GAC and anthracite samples were added to sterile saline (NaCl, 8.5 g/L) and ultrasonicated at 38 kHz, 600 W three times with 20 min exposure and 5 min intervals to suspend the biofilms (Wan *et al*., 2019). The biofilm suspensions, influents and effluents were filtered through 0.22 μm mixed cellulose ester membrane filters (Millipore, UK) by a vacuum filtration apparatus. All of the membranes were stored at - 20 ºC. Genomic DNA was extracted using the FastDNA Spin Kit for Soil (MP Biomedicals, UK) according to the manufacturers' instructions. The concentration of the purified DNA was quantified spectrophotometrically using the NanoDrop and stored at - 85 ºC until further analysis. In-house qPCR assays were established to quantify the target ARGs and two integron genes. Details of qPCR procedures were as described in a previous study by the authors (Xu *et al*., 2019).

2.3 Bacterial community structure analysis

DNA samples extracted from surface layer biofilms which collected at the end of system run (before backwashing/cleaning) were sent for amplicon sequencing using the Illumina Hiseq2500 platform (Novogene, Beijing, China). The V3-V4 region of the *16S rRNA*

gene was selected for amplification with primers 341F: CCTAYGGGRBGCASCAG and 806R: GGACTACNNGGGTATCTAAT. Paired-end reads were merged using FLASH (V1.2.7, http://ccb.jhu.edu/software/FLASH/). Raw tags were filtered according to the Quantitative Insights Into Microbial Ecology (QIIME, V1.7.0, http://qiime.org/index.html) quality controlled process in order to obtain the high-quality clean tags. Analysis of the generated high-quality sequences was performed by Uparse software (v7.0.1001, http://drive5.com/uparse/). Sequences with ≥97% similarity were assigned to the same operational taxonomic unit (OTU). Representative sequence for each OTU was classified phylogenetically and assigned to a taxonomic identity using the Ribosomal Database Project (RDP) classifier (Version 2.2, http://sourceforge.net/projects/rdp-classifier/).

2.4 Horizontal conjugative transfer experiment

The donor strain used was *E. coli* J53, which harbours the conjugative RP1 plasmid that confers resistance to ampicillin (encoded by bla_{TEM}), tetracycline (encoded by *tetA* and *tetR*) and kanamycin (encoded by *aphA*). The *E. coli* HB 101 strain resistant to streptomycin was used as the recipient. The donor strain was pre-cultured in Luria-Bertani (LB) broth or agar supplemented with 100 mg/L ampicillin, 10 mg/L tetracycline, and 50 mg/L kanamycin; while the recipient strain was pre-cultured in LB broth or agar supplemented with 30 mg/L streptomycin. Recipients carrying the RP1 plasmid were recognised as transconjugants and cultured in LB broth or agar supplemented with 100 mg/L ampicillin, 10 mg/L tetracycline, 50 mg/L kanamycin, and 30 mg/L streptomycin.

Two sets of biofiltration systems (Set A and Set B) were setup at bench-scale (Figure 2), each consisting of three columns (inner diameter 2 cm) loaded with sand, GAC and anthracite up to 7 cm. All the materials, including filter media, feedwater reservoir, tubing and columns were autoclaved prior to system set-up. The six biofilters were operated in parallel under identical conditions at a hydraulic retention time of 0.06 m/h for two weeks. Set A was fed with LB broth (1:1000 diluted, dissolved organic carbon = 6 mg/L) spiked with the five target antibiotics at 2 µg/L, while Set B was only fed with diluted LB broth. Both, Set A and B,

were inoculated with equal amount of fresh culture of *E. coli* J53 and HB101 at approximately 1.0×10^7 CFU/mL for two weeks. After two weeks' operation, the system was backwashed once by pumping sterile water in counter current through the columns at 30% fluidisation for 5 min. Influent, effluent and surface media samples were collected 24 h after first inoculation and then every two days thereafter. Once collected, media samples were suspended in sterile saline and then ultrasonicated at 38 kHz for 20 min to wash off the bacteria attached to the media surface. Influent, effluent and media bacteria suspension samples were serially diluted and plated on selective LB agar to count the numbers of donors, recipients and transconjugants. All plates were incubated at 37 ºC for 24 h. The conjugative transfer frequency in media and aqueous samples was then calculated based on the numbers of transconjugants per recipient cell. Colony PCR was conducted to determine the RP1 plasmid genotype in transconjugants (details are provided in the SI). *E. coli* HB101 was plated onto selective LB agar separately as negative controls throughout the study.

2.5 Statistical analysis

The absolute abundance or concentration of ARGs indicated the ARG copy numbers per gram in medium samples (copies/g) or per litre in influent/effluent samples (copies/L). The relative abundance of ARG was calculated based on the ARG copies normalised to the number of copies of the *16S rRNA* gene. The number of different ARGs detected was expressed as the richness of ARGs. Mean and standard deviation calculations were performed with Microsoft Excel 2016. One-way analysis of variation (ANOVA), Pearson correlation analysis and ARGs' profile heatmap were performed using OriginPro 2018. Principal coordinate analysis (PCoA) based on Bray-Curtis distance was utilised to evaluate the bacterial community profiles between different biofilm samples. Redundancy analysis (RDA) was performed to analyse the correlation between ARGs and bacterial communities (considered as the environmental factor). Variation partitioning analysis (VPA) was performed to explore the contributions of integrons and bacterial communities to the variations of ARGs. PCoA, RDA and VPA were performed using Canoco 5.0 software (USA). Venn diagram

193 analysis was performed to assess the numbers of shared and unique OTUs in each biofilm
194 sample. OriginPro 2018 was used to draw histogram, line graphs and Venn diagram.

3. Results and discussion

3.1 Behaviour of ARGs and integron genes during biofiltration

3.1.1 Overview of ARGs and integron genes in biofilms

A total of 64 biofilm samples were collected from different sampling sites at 4 weeks (before antibiotics spike) and 11 weeks (after spiking and before backwashing/cleaning) of the biofilter run. For a better understanding of the sampling positions, M0, M8, M17 and M20 referred to media samples collected at 0 cm, 8 cm, 17 cm, and 20 cm along the column, respectively. An overview of the absolute abundance of the *16S rRNA* gene, ARGs and integrons are shown in Figure S3. Mean values of the absolute abundance of ARGs were 2.04 × 10^6, 1.06 × 10^6, and 6.81 × 10^5 copies/g in sand, GAC and anthracite biofilms, respectively. Among the ARGs present, bla_{TEM} was the most abundant resistance gene (4.29 × 10^6 copies/g), followed by *sul 1* (3.23 × 10^6 copies/g) and *tetG* (1.27 × 10^6 copies/g). The trimethoprim resistance gene *dfrA12* had the lowest abundance (7.05 × 10^2 copies/g). No statistical differences ($p > 0.05$) in total ARG abundance were found between the duplicate columns or between 4-week and 11-week biofilm samples. A decrease in ARG concentrations and richness with depth was observed among the same media type (Figure S4). The absolute abundance of ARGs were positively correlated to the *16S rRNA* gene and the integrons (Figure S5-a) in biofilm samples.

Figure 3 shows an overview of the relative abundance of ARGs and integrons in all biofilms. The relative abundance of ARGs increased significantly ($p < 0.01$) with increasing depth (from M0 to M17) while the absolute concentration decreased in sand biofilms. This may due to the amount of microbial biomass attached to the surface layer was much greater than the deeper layer, evidenced by an average of 1.4-log and 1.2-log higher of the absolute abundance of *16S rRNA* and ARGs, respectively, in the surface than in the deeper layer biofilms (Figure S3). These observations are consistent with the study of Wan *et al.* (2019) on sand biofilm. In the GAC biofilm samples, the overall ARG concentrations ranged between 5.65 × 10^6 and 1.87 × 10^7 copies/g in the surface layer biofilms and between 7.94 × 10^4 to

222 2.13×10^6 copies/g in the lower layers. It should be noted that after the addition of antibiotics,
223 the relative abundance of integron genes increased significantly ($p < 0.01$) in GAC biofilms,
224 raising the mean concentration from 6.91×10^4 copies/g (week 4) to 8.27×10^5 copies/g (week
225 11). Although no reference of ARG variation within the GAC biofilm over time is available,
226 research focused on ARG prevalence in DWTPs has shown that the biofilm on a GAC filter
227 influenced ARG profiles in the filtered water and the diversity of ARGs in water increased after
228 GAC filtration (Zheng *et al*., 2018). This is also confirmed by Xu *et al*. (2016), where the
229 number of detected ARGs raised significantly from 76 to 150 after GAC treatment. The
230 enhanced ARG and integron levels in the GAC biofilms observed in this study suggest that
231 they might pose a potential impact on the ARG profile of the filtered water. For the GSB, biofilm
232 collected at a depth of 17 cm (M17) was from GAC media and at 8 cm and 20 cm depth (M8
233 and M20) were from sand. Despite the lower level of ARGs abundance observed, the relative
234 abundance of ARGs in the GAC biofilm was the highest compared to sand in week 11 samples.
235 This may be due to the adsorption capacity of GAC on antibiotics which could exert a selective
236 pressure for the resistant bacteria in the biofilm, contributing to an enhanced relative
237 abundance. For the ASB, M8 and M17 represented anthracite biofilms, and M20 was a sand
238 biofilm. No difference of the relative abundance of ARGs was found between the two non-
239 adsorptive media.

240 **3.1.2 Behaviour of ARGs and integron genes in influent and effluent**

241 Figure 4 shows an overview of the ARGs and integrons abundance in the influent and
242 effluent samples. No statistical differences ($p > 0.05$) were found between the duplicate
243 biofilters. For the absolute abundance, ARGs showed positive correlations with both the *16S*
244 *rRNA* gene and integrons in water samples (Figure S5-b). The overall ARG concentration
245 ranged from 2.96×10^6 to 1.86×10^8 copies/L in the influent and from 1.73×10^5 to 7.36×10^7
246 copies/L in the effluents. After filtration, 0.76-log, 0.66-log, 1.29-log and 1.15-log reductions in
247 ARG copy numbers were observed for SB, GB, GSB and ASB, respectively.

Although the absolute abundance of ARGs decreased, the normalised ARGs copy numbers showed an increasing trend in the filtered water. *IntI 1* also showed a trend of increasing in relative abundance, although this trend fluctuated for duplicate biofilters. The above findings are consistent with the findings in DWTPs, where the relative abundance of ARGs increased after sand or GAC biofiltration (Xu *et al*., 2016; Zheng *et al*., 2018). This may due to the releasing of the attached biofilm cells into the water, or the gene exchanges occurred between the microbes in biofilm and water. In general, the trends for the reduction of ARGs in GAC-associated biofilters were more stable than those in the biofilters using non-adsorptive media over time (Figure S6). Backwashing and cleaning of biofilters did not affect the removal of ARGs significantly, especially for the GAC biofilter. In previous study, the backwashing of GAC biofilter has shown no considerable effect on the bacterial population and diversity in biofilms (Kim *et al*., 2014), which might allow the GAC biofilter to function in a stable manner in terms of ARG reduction.

3.1.3 Comparisons of ARGs profiles in biofilm and aqueous samples

Raw water samples were included to provide background information on the ARGs profile. In general, the concentration of ARGs in raw water ranged from 10^3 to 10^8 copies/L, which is comparable to ARGs levels (10^3 to 10^7 copies/L) reported by the authors in a previous study investigating the same types of surface water in London (Xu *et al*., 2019). The levels of ARGs/integron abundance fluctuated over time, and 10 out of 15 target genes were present in all batch samples. A heatmap showing the profile of the relative abundance of ARGs in raw water, influent, effluent, surface and lower layer biofilm samples is shown in Figure 5. Biofilm samples represented a higher level of the relative abundance of ARGs (6.61×10^{-3} on average) than in the aqueous samples (2.12×10^{-3} on average). Among the ARGs present, *sul 1* was the most persistent resistance gene in all types of sample, and the β-lactam resistance genes (*bla*) accumulated considerably more (20-fold) in biofilms than in the aqueous samples. The concentrations of *16S rRNA* gene, individual ARG, and integrons in raw water samples are provided in Figure S7.

Comparisons of ARGs between biofilms collected at different depths (Figure S8) showed that the surface layer biofilms (M0), which had the highest absolute abundance and richness of ARGs, had the lowest relative abundance of ARG ($p < 0.01$) compared to the deeper layer biofilms (M8, M17 and M20). This indicates that the proportion of ARGs-carrying bacteria was greater in the lower position. Little research has been conducted on the behavioural mechanisms of ARGs in different depths of filter columns, nor has this been investigated in the context of the impact of different types of media on ARG variation. Wan *et al.* (2019) have found a similar trend of an increasing relative abundance in ARGs in the lower depths of sand biofilms, which is possibly due to the consumption of organic carbon along the filter column. In general, the concentration of dissolved organic carbon (DOC) decreases with increasing depth in the filter bed. A previous study has found that the DOC concentration decreased more rapidly in the 0-10 cm layer of the sand, GAC and anthracite filter bed, where the removal of DOC accounted for > 50% of the overall removal (Zhang *et al*., 2015). As the resistant bacteria tend to be more competitive under poor nutrient conditions (Lin *et al*., 2018), it is likely that the low level of carbon source in the lower depth of filter bed could be a limiting factor for the growth of susceptible strains, resulting in a higher relative abundance of ARGs in the deeper biofilms.

Significant positive correlations ($P < 0.05$) were found between all types of samples (Table S1), indicating that the distributions of ARGs in the filtered water were affected by both raw water and biofilms formed in the filter column. In biofilm samples, *intI 1* displayed significant correlations with the absolute abundances of two classes of ARGs (∑*sul* and ∑*tet*) ($r = 0.60$ and 0.44, respectively, $P < 0.01$, Table S2). And in aqueous samples, *intI 1* was found to significantly relate to the absolute abundances of three classes of ARGs (∑*sul*, ∑*tet* and ∑*bla*) ($r = 0.50$, 0.35 and 0.91, respectively, $P < 0.05$, Table S3). In addition, *intI 2* had strong and significant relationships with *dfrA*1 and *dfrA*12 ($r = 0.43$ and 0.53, respectively, $P < 0.05$) in aqueous samples, as well as with all ARGs ($r = 0.64$, $P < 0.01$). The significant correlations observed between integron genes with ARGs indicated that class 1 and class 2

integrons play important roles in the dissemination of ARGs in the biofilms and filtered water through HGT.

3.2 Bacterial community in filter biofilm

Bacterial community structure was investigated in the surface layer biofilms formed on sand, GAC and anthracite after 11 weeks' operation. A total of 1,069,777 tags with an average of 116,226 high quality tags per sample were obtained. These sequences were clustered into 3313 OTUs. The dominant phyla in all samples were *Proteobacteria* (51.9%), *Actinobacteria* (13.5%), *Bacteroidetes* (8.5%), *Firmicutes* (7.6%), and *Acidobacteria* (5.2%), accounting 87% of the total bacterial communities (Figure 6a). No statistical differences were found between duplicate biofilters at the phylum level. *Alphaproteobacteria* and *Betaproteobacteria* were more predominant in GAC than in sand and anthracite at the class level (Figure S9). As the second most abundant phylum, *Actinobacteria* were more abundant in sand biofilm communities. *Bacteroidetes* was the third most abundant phylum, which was attributed to its member classes *Sphingobacteriia* and *Cytophagia*. The *Firmicutes* were primarily composed of class *Clostridia*, which occupied 5.7%, 4.4% and 3.1% in sand, GAC and anthracite biofilms, respectively. Previous research has also reported similarities in microbial taxa in biofilters (Haig *et al*., 2014; Li *et al*., 2019), but the corresponding percentage differed by filter type (e.g., relative abundance of *Proteobacteria*: GAC > sand > anthracite). At genus level, *Sulfuritalea* and *Sphingobium*, which belong to the *Proteobacteria*, were the dominant genus in sand and GAC biofilms, respectively (Figure S10). *Bacillus*, within the *Firmicutes*, was the most abundant genus in anthracite. The genera *Bacillus*, *Legionella*, *Mycobacterium*, and *Pseudomonas* were present in all biofilm samples, and their relative abundance was up to 8.6% in one of the anthracite biofilms (Table S4). These opportunistic human pathogens found in surface layer biofilms could be unintentionally released to the filtered water and pose potential risks to distribution waters.

PCoA showed that the duplicate biofilters were clustered together and separated from other biofilter type (Figure 6b). This indicated that the filter substrate plays an important role in shaping the bacterial community structure in biofilms. The Venn diagram shows that 1453 OUTs were shared between all biofilms (Figure 6c). Total OTUs per biofilter type was 3824, 3210, 3156, and 2377 in SB, GB, GSB and ASB, respectively. A higher number of 4901 OTUs was obtained from the sand biofilms, according to Wan *et al*. (2019), which reflects the differences in the indigenous bacterial community in the sand filter. Consistent with the present study, previous research has also found greater numbers of OTUs in GAC filters than in anthracite filters (Shirey *et al*., 2012). In particular, 2390 OTUs were shared between the sand biofilms (SB and GSB) and 1716 OTUs were shared between the carbon-based substrates (GB and ASB). The number of the unshared OTUs were the highest (662 OTUs) in SB and the lowest (187 OTUs) in ASB, respectively, revealing that more unique bacteria were identified in SB.

3.3 Links between ARGs, integrons and the bacterial community

The first two axes in RDA (Figure 7a) showed that 90.6% of the variance in ARGs could be explained by the selected variables. Most chosen ARGs correlated with *Acidobacteria* and *Nitrospirae*, which accounted for 5.2% and 2.0% of the bacterial phyla in biofilm communities, respectively. In addition to the bacterial community, RDA analysis further confirmed that integron genes contributed to the variation of most ARGs in surface layer biofilms. It should be noted that GAC media were more closely related to *intI 1* than other biofilters, suggesting a greater extent of integron-mediated ARG exchange in GB. The superior adsorption capacity and higher surface area of GAC may lead to an accumulation of antibiotics within the biofilm and consequently exert a selective potential. Pearson correlations between the relative abundance of ARGs and major bacterial phyla are summarised in Table S5.

Results from RDA are generally not comparable with other studies as the experimental conditions were different. For instance, Huerta *et al*. (2013) found that bla_{TEM} was associated with *Actinobacteria* in water samples collected from man-made reservoirs, which is consistent

with the observations in this study. However, in their study, *ermB* was found to be associated with *Firmicutes* in water and with *Actinobacteria* in sediment samples, while this gene was correlated to *Proteobacteria* in the present study. To differentiate the effects of the bacterial community and integrons on the change of ARG composition, VPA showed that a total of 77.7% of the variance in ARGs could be explained by selected variables in the biofilm samples (Figure 7b). The bacterial community explained the largest variation (55.3%), which is similar to the contributions of 50.44% and 57.22% observed in previous drinking water-related research (Jia *et al*., 2015; Zheng *et al*., 2018). The integron explained 7.9% of the variation of ARGs, and the joint effect of bacterial community and integron contributed 14.5% on the ARG variation. The low contribution of the integron indicated that other HGT vehicles (e.g. transposons) may also contribute to the propagation of ARGs in the biofilms.

Previous research and the present study considered the mixture of surface filter media and the upper slimy layer as the surface biofilm samples, however, they may represent different levels of risk in ARG pollution. As the surface biofilm shapes the bacterial community in the drinking water microbiome (Pinto *et al*., 2012; Pompei *et al*., 2017), it is important to understand which part of the biofilm exerts a higher influence on ARG proliferation during biofiltration. This could further provide an insight into biofilter management strategies and appropriate ways for the disposal of used media. For instance, considering the persistence of ARGs during biofiltration process, land application of biofilter waste products may act as an environmental exposure route for trace levels of ARGs and introduce a reservoir for ARG pollution in previously unexposed regions.

3.4 Horizontal conjugative transfer occurred during biofiltration

3.4.1 Plasmid conjugative transfer in biofilms

Figure 8 shows that the GAC media had the highest RP1 plasmid transfer frequency (2.60×10^{-5} on average), followed by anthracite (5.31×10^{-6} on average) and sand (2.47×10^{-6} on average). The transfer frequency in the sand biofilm increased steadily from 4.41×10^{-8} on day 1 to 6.04×10^{-6} on day 5, then plateaued between 10^{-6} to 10^{-5} after a week, indicating

the bacterial attachment and detachment remained dynamically balanced in the sand biofilm. The high surface area and unique pore structure of GAC may induce bacterial collision and attachment, contributing to more frequent conjugation. Anthracite biofilm showed a fluctuating but relatively stable transfer frequency compared to sand and GAC biofilm. Plasmid conjugative transfer occurred at frequencies up to 3.69×10^{-1} in a biofilm reactor (Ehlers and Bouwer, 1999), which is much higher than the levels observed in the present study.

Transfer frequencies reduced significantly ($p < 0.01$) in all of the media samples after backwashing was conducted on day 14. The conjugative transfer frequency in biofilms was 1.47×10^{-5} and 1.15×10^{-5} (on average) in Set A and B, respectively, with no statistical difference ($p > 0.05$). It is possible that the antibiotic spike concentration (2 μg/L) was not sufficient to exhibit a selective pressure on bacterial strains to induce the horizontal conjugative transfer in biofilms. Lundström *et al.* (2016) reported that 1 μg/L tetracycline is sufficient to select for the *tetA* gene in freshwater biofilms but not for phenotypic resistance, which was observed at a higher level of 10 μg/L. The minimal selective concentration for resistant bacteria was predicted at 2 μg/L for amoxicillin and clarithromycin; 4 μg/L for oxytetracycline; 8 μg/L for trimethoprim; and 125 μg/L for sulfamethoxazole (Bengtsson-Palme and Larsson, 2016). The concentration of 2 μg/L used in this study was likely to be too low for the selection of phenotypically resistant recipients. However, under real drinking water treatment conditions, microbes are generally exposed not only to trace levels of antibiotics, but also to other micropollutant residues such as heavy metals and disinfection by-products, which could co-select for mobile genetic elements carrying multiple resistant genes, contributing to the spread of resistance in both biofilm and water samples (Baker-Austin *et al*., 2006; Li *et al*., 2016; Lv *et al*., 2014).

3.4.2 Plasmid conjugative transfer in aqueous samples

The average removal of *E. coli* strains was 55.1% by the biofilters during the two-week's operation (Figure S11). The numbers of *E. coli* cells in the filtered water were positively correlated to the numbers in the influent ($R^2 > 0.89$, $P < 0.01$) and independent to the numbers

found in the corresponding media samples, suggesting that the donor and recipient behaved differently in stationary phase (media surface) and planktonic phase (influent and effluent), which could consequently affect the conjugative transfer. The transfer frequency of the RP1 plasmid in the influent and effluent samples, with an average transfer frequency of 3.17×10^{-6} in the influents and 1.86×10^{-5} in the effluents during days 1 to 13 (see Table S6 for full details). These levels were similar to those described by Qiu *et al*. (2012), where the natural conjugative transfer frequency of RP4 (a plasmid similar to RP1) ranged from 0.15×10^{-6} to 2.0×10^{-6} in water after an 8-h mating time. Apart from the spontaneous occurrence of conjugation, the enhanced transfer rate in the filtered water was probably due to the 'escape' of transconjugants from the media surface. Interestingly, on day 1, transconjugants were absent in GAC media while present in one of the GAC filtered water samples, and an opposite trend was found in the sand biofilters. This further confirmed that the mechanisms underlying the conjugative transfers in media surface and influent/effluent were different. Backwashing increased the likelihood of escape of transconjugants, evidenced by the detection frequency of transconjugants increased from 0-33.3% (day 1-13) to 66.7% (day 14) in the effluents.

3.4.3 Mechanisms underlying the effect of biofiltration on plasmid conjugative transfer

The donor and recipient have the ability to attach, form and integrate into a biofilm on the media surface, providing a stationary phase (biofilm) in a continuous feed (planktonic phase) (Lundström *et al*., 2016). Based on the findings of this study, we inferred that RP1 transfer might occur in three different contexts (Figure 9):

1) stationary phase, where transfer takes place either on the surface or inside the media (e.g. GAC micropores). In the biofilm, the close contact of donor and recipient numbers prompted plasmid transfer;
2) stationary-planktonic phase, where the transfer occurs between the bacteria retained in the biofilm and the bacteria in the feed water flowing through the media. A lower hydraulic loading rate was used throughout this study, allowing the microbes in the

feedwater to have the opportunity to interact with microbes in the biofilm, resulting in conjugative transfer of RP1;

3) planktonic phase, where the transfer might occur in the feed (before filtration), during filtration, or in the effluent (after filtration). The frequency of transfer in the planktonic phase is expected to be much lower than that in other two forms.

For the occurrence of conjugative transfer in liquid environments, donors and recipients must make physical contact, attach, and then conjugate before detachment occurs (Zhong *et al*., 2010). Theoretically, it is not possible to distinguish between the three contexts. Bacteria can be mobilised between the biofilm and water (e.g. biofilm detachment) during biofiltration. In this study, we assumed that the occurrence of plasmid conjugative transfer in stationary phase mainly affected the results obtained from media samples and partially affected the results obtained for the effluents. To rule out spontaneous mutation of recipient strains during biofiltration and confirm the transfer of RP1 plasmid, one to three suspected transconjugants were randomly chosen and tested by PCR (Figure S12). All of the transconjugants were confirmed to have bla_{TEM} and *tetA*. The result indicated that all colonies had acquired RP1 plasmids and no spontaneous mutation of recipient strains was observed.

Despite the concentration of donor and recipient cells being the same in the inoculum, higher numbers of recipients were consistently found in media samples. This indicated that the biofilm-forming ability of the recipient is stronger than that of the donor strain, which is key to conjugative transfer. Zheng *et al.* (2018) confirmed that conjugative transfer between the same bacterial genera in a GAC biofilter is regulated by quorum sensing, a communication system used by bacteria which can control the degree of biofilm formation and determines the behaviour of biofilm communities (Parsek and Greenberg, 2005). In the biofiltration process, when the donor and recipient accumulate on the media surface, they could emit and sense chemical signals which favour the plasmid transfer between *E. coli* strains (Zheng *et al*., 2018). In addition to the biofilm developed on GAC surface, the unique pore structures could capture more bacterial cells and facilitate cell-to-cell contact, contributing to the high transfer frequency seen in GAC media.

4 Conclusions

- Biofiltration leads to an increase in the relative abundance of ARGs and integrons in the filtered water.
- The proportion of ARG-carrying bacteria was greater in the deeper layers of biofilms compared to surface layer biofilms, and biofilms represented higher risk of ARG pollution than in the aqueous samples.
- The ARGs investigated were correlated to *Proteobacteria*, *Acidobacteria* and *Nitrospirae*. The bacterial community explained the largest variation (55.3%) of ARGs in the surface layer biofilms.
- Compared to sand and anthracite, GAC media facilitated horizontal transfer of ARGs in biofilms.

Overall, this study provides an insight into biofilter management strategies and appropriate ways for the disposal of used media. Furthermore, the results could be used in assessing ARG-related risks in drinking water treatment and to provide useful references for researchers.

Declaration of Competing Interests

No conflict of interest declared.

Acknowledgement

The donor strain *E. coli* J53 was provided by Prof. Matthew Avison and Dr Jacqueline Findlay from University of Bristol; the recipient *E. coli* HB 101 was gifted by Prof. Laura Piddock and Dr Maria Laura Ciusa from University of Birmingham. Miss Like Xu is sponsored by UCL Dean's Prize and China Scholarship Council (CSC, No. 201506320207). Thanks to the manager in the Regent's Park for authorising the water sampling.

References

Baker-Austin, C., Wright, M.S., Stepanauskas, R. and McArthur, J.V. 2006. Co-selection of antibiotic and metal resistance. Trends Microbiol. 14(4), 176-182.

Bengtsson-Palme, J. and Larsson, D.G.J. 2016. Concentrations of antibiotics predicted to select for resistant bacteria: Proposed limits for environmental regulation. Environ. Int. 86, 140-149.

Chen, B., Yuan, K., Chen, X., Yang, Y., Zhang, T., Wang, Y., Luan, T., Zou, S. and Li, X. 2016. Metagenomic analysis revealing antibiotic resistance genes (ARGs) and their genetic compartments in the Tibetan environment. Environ. Sci. Technol. 50(13), 6670-6679.

D'Alessio, M., Yoneyama, B., Kirs, M., Kisand, V. and Ray, C. 2015. Pharmaceutically active compounds: Their removal during slow sand filtration and their impact on slow sand filtration bacterial removal. Sci. Total Environ. 524, 124-135.

de Vera, G.A., Gerrity, D., Stoker, M., Frehner, W. and Wert, E.C. 2018. Impact of upstream chlorination on filter performance and microbial community structure of GAC and anthracite biofilters. Environ. Sci.: Water Res. Technol. 4(8), 1133-1144.

Ehlers, L. and Bouwer, E.J. 1999. RP4 plasmid transfer among species of *Pseudomonas* in a biofilm reactor. Water Sci. Technol. 39(7), 163–171.

Farkas, A., Butiuc-Keul, A., Ciataras, D., Neamtu, C., Craciunas, C., Podar, D. and Dragan-Bularda, M. 2013. Microbiological contamination and resistance genes in biofilms occurring during the drinking water treatment process. Sci. Total Environ. 443, 932-938.

Gao, P.P., Mao, D.Q., Luo, Y., Wang, L.M., Xu, B.J. and Xu, L. 2012. Occurrence of sulfonamide and tetracycline-resistant bacteria and resistance genes in aquaculture environment. Water Res. 46(7), 2355-2364.

Haig, S.J., Quince, C., Davies, R.L., Dorea, C.C. and Collins, G. 2014. Replicating the microbial community and water quality performance of full-scale slow sand filters in laboratory-scale filters. Water Res. 61, 141-151.

511 Huerta, B., Marti, E., Gros, M., Lopez, P., Pompeo, M., Armengol, J., Barcelo, D., Balcazar,
512 J.L., Rodriguez-Mozaz, S. and Marce, R. 2013. Exploring the links between antibiotic
513 occurrence, antibiotic resistance, and bacterial communities in water supply reservoirs.
514 Sci. Total Environ. 456, 161-170.
515 Huisman, L. and Wood, W.E. 1974. Slow Sand Filtration. World Health Organization, Geneva
516 Switzerland.
517 Jia, S., Shi, P., Hu, Q., Li, B., Zhang, T. and Zhang, X.X. 2015. Bacterial community shift
518 drives antibiotic resistance promotion during drinking water chlorination. Environ. Sci.
519 Technol. 49(20), 12271-12279.
520 Kim, T.G., Yun, J., Hong, S.H. and Cho, K.S. 2014. Effects of water temperature and
521 backwashing on bacterial population and community in a biological activated carbon
522 process at a water treatment plant. Appl. Microbiol. Biot. 98(3), 1417-1427.
523 Letterman, R.D. 1991. Filtration Strategies to Meet the Surface Water Treatment Rule.
524 American Water Works Association, Denver, CO.
525 Li, D., Zeng, S.Y., He, M. and Gu, A.Z. 2016. Water disinfection byproducts induce antibiotic
526 resistance-role of environmental pollutants in resistance phenomena. Environ. Sci.
527 Technol. 50(6), 3193-3201.
528 Li, J., Han, X., Brandt, B.W., Zhou, Q., Ciric, L. and Campos, L.C. 2019. Physico-chemical
529 and biological aspects of a serially connected lab-scale constructed wetland-stabilization
530 tank-GAC slow sand filtration system during removal of selected PPCPs. Chem. Eng. J.
531 369, 1109-1118.
532 Lin, W., Zeng, J., Wan, K., Lv, L., Guo, L., Li, X. and Yu, X. 2018. Reduction of the fitness cost
533 of antibiotic resistance caused by chromosomal mutations under poor nutrient conditions.
534 Environ. Int. 120, 63-71.
535 Liu, B., Gu, L., Yu, X., Yu, G.Z., Zhang, H.N. and Xu, J.L. 2012. Dissolved organic nitrogen
536 (DON) profile during backwashing cycle of drinking water biofiltration. Sci. Total Environ.
537 414, 508-514.

538 Liu, L.M., Su, J.Q., Guo, Y.Y., Wilkinson, D.M., Liu, Z.W., Zhu, Y.G. and Yang, J. 2018. Large-
539 scale biogeographical patterns of bacterial antibiotic resistome in the waterbodies of China.
540 Environ. Int. 117, 292-299.
541 Lundström, S.V., Östman, M., Bengtsson-Palme, J., Rutgersson, C., Thoudal, M., Sircar, T.,
542 Blanck, H., Eriksson, K.M., Tysklind, M., Flach, C.-F. and Larsson, D.G.J. 2016. Minimal
543 selective concentrations of tetracycline in complex aquatic bacterial biofilms. Sci. Total
544 Environ. 553, 587-595.
545 Lv, L., Jiang, T., Zhang, S.H. and Yu, X. 2014. Exposure to mutagenic disinfection byproducts
546 leads to increase of antibiotic resistance in *Pseudomonas aeruginosa*. Environ. Sci.
547 Technol. 48(14), 8188-8195.
548 Parsek, M.R. and Greenberg, E.P. 2005. Sociomicrobiology: the connections between
549 quorum sensing and biofilms. Trends Microbiol. 13(1), 27-33.
550 Pinto, A.J., Xi, C.W. and Raskin, L. 2012. Bacterial community structure in the drinking water
551 microbiome is governed by filtration processes. Environ. Sci. Technol. 46(16), 8851-8859.
552 Pompei, C.M.E., Ciric, L., Canales, M., Karu, K., Vieira, E.M. and Campos, L.C. 2017.
553 Influence of PPCPs on the performance of intermittently operated slow sand filters for
554 household water purification. Sci. Total Environ. 581-582, 174-185.
555 Qiu, Z.G., Yu, Y.M., Chen, Z.L., Jin, M., Yang, D., Zhao, Z.G., Wang, J.F., Shen, Z.Q., Wang,
556 X.W., Qian, D., Huang, A.H., Zhang, B.C. and Li, J.W. 2012. Nanoalumina promotes the
557 horizontal transfer of multiresistance genes mediated by plasmids across genera. Proc.
558 Natl. Acad. Sci. 109(13), 4944-4949.
559 Reungoat, J., Escher, B.I., Macova, M. and Keller, J. 2011. Biofiltration of wastewater
560 treatment plant effluent: Effective removal of pharmaceuticals and personal care products
561 and reduction of toxicity. Water Res. 45(9), 2751-2762.
562 Schlüter, A., Szczepanowski, R., Pühler, A. and Top, E.M. 2007. Genomics of IncP-1
563 antibiotic resistance plasmids isolated from wastewater treatment plants provides
564 evidence for a widely accessible drug resistance gene pool. Fems. Microbiol. Rev. 31(4),
565 449-477.

566 Schwartz, T., Kohnen, W., Jansen, B. and Obst, U. 2003. Detection of antibiotic-resistant
567 bacteria and their resistance genes in wastewater, surface water, and drinking water
568 biofilms. Fems. Microbiol. Ecol. 43(3), 325-335.
569 Shirey, T.B., Thacker, R.W. and Olson, J.B. 2012. Composition and stability of bacterial
570 communities associated with granular activated carbon and anthracite filters in a pilot
571 scale municipal drinking water treatment facility. J. Water Health. 10(2), 244-255.
572 Wan, K., Zhang, M.L., Ye, C.S., Lin, W.F., Guo, L.Z., Chen, S. and Yu, X. 2019. Organic
573 carbon: An overlooked factor that determines the antibiotic resistome in drinking water
574 sand filter biofilm. Environ. Int. 125, 117-124.
575 Wang, F.H., Qiao, M., Su, J.Q., Chen, Z., Zhou, X. and Zhu, Y.G. 2014. High throughput
576 profiling of antibiotic resistance genes in urban park soils with reclaimed water irrigation.
577 Environ. Sci. Technol. 48(16), 9079-9085.
578 Xu, L., Chen, H., Canales, M. and Ciric, L. 2019. Use of synthesized double-stranded gene
579 fragments as qPCR standards for the quantification of antibiotic resistance genes. J.
580 Microbiol. Meth. 164, 105670.
581 Xu, L., Ouyang, W., Qian, Y., Su, C., Su, J. and Chen, H. 2016. High-throughput profiling of
582 antibiotic resistance genes in drinking water treatment plants and distribution systems.
583 Environ. Pollut. 213, 119-126.
584 Zhang, H.N., Zhang, K.F., Jin, H.X., Gu, L. and Yu, X. 2015. Variations in dissolved organic
585 nitrogen concentration in biofilters with different media during drinking water treatment.
586 Chemosphere. 139, 652-658.
587 Zhang, X.X., Zhang, T. and Fang, H. 2009. Antibiotic resistance genes in water environment.
588 Appl. Microbiol. Biot. 82(3), 397-414.
589 Zheng, J., Chen, T. and Chen, H. 2018. Antibiotic resistome promotion in drinking water
590 during biological activated carbon treatment: Is it influenced by quorum sensing? Sci. Total
591 Environ. 612, 1-8.
592 Zhong, X., Krol, J.E., Top, E.M. and Krone, S.M. 2010. Accounting for mating pair formation
593 in plasmid population dynamics. J. Theor. Biol. 262(4), 711-719.

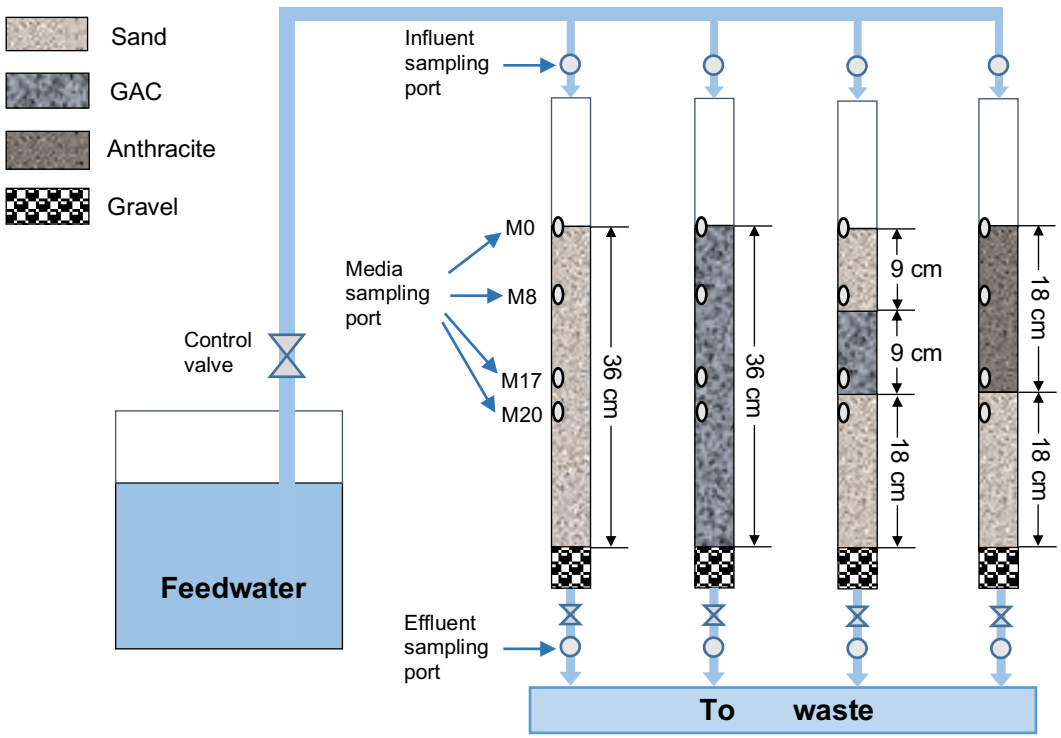

Figure 1 Schematic of biofilter composition. Sampling ports are denoted by. M0, M8, M17 and M20 refer to media (biofilm) samples collected at 0, 8 cm, 17 cm and 20 cm along the column. SB: sand biofilter; GB: GAC biofilter; GSB: GAC sandwich biofilter; ASB: anthracite-sand biofilter.

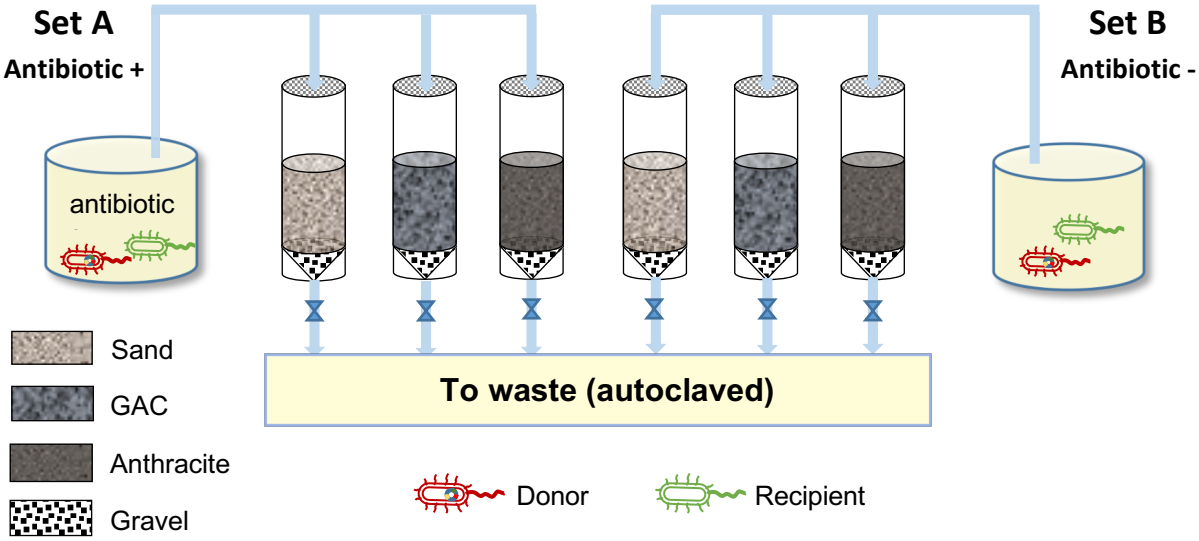

Figure 2 Bench-scale biofilters schematic.

Set A: biofilters exposed to antibiotics at 2 µg/L; Set B: biofilters without antibiotics addition.

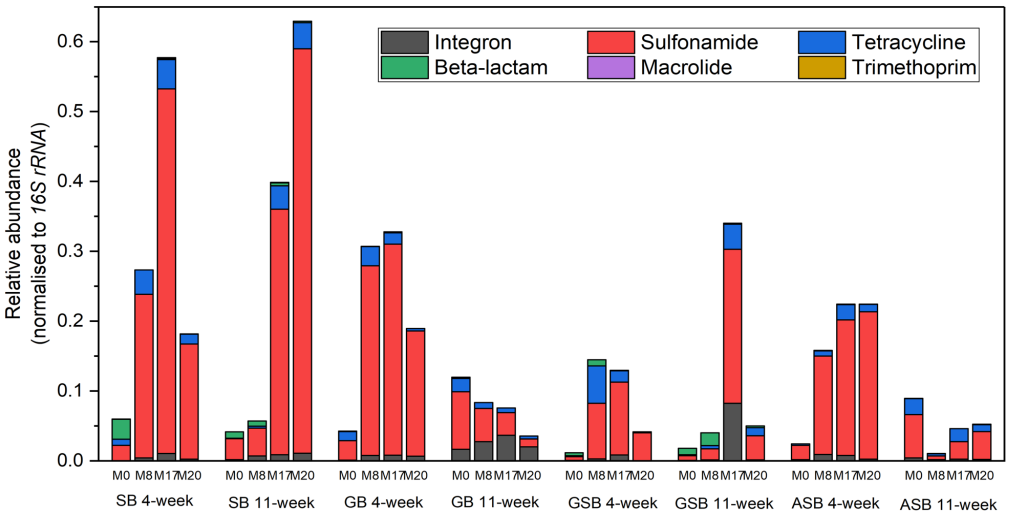

Figure 3 Relative abundance of ARG categories and integron at each sampling site of biofilter. Sample M0, M8, M17 and M20 refer to biofilm collected at different sampling sites (0, 8, 17, and 20 cm). SB: sand biofilter; GB: GAC biofilter; GSB: GAC sandwich biofilter; ASB: anthracite-sand biofilter.

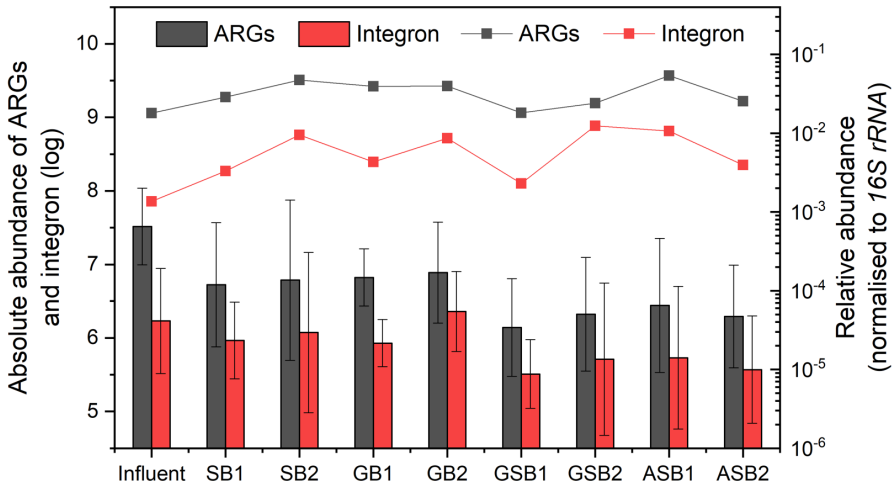

Figure 4 Absolute abundance (bar chart, left Y-axis) and relative abundance (line and symbol, right Y-axis) of ARGs and integrons in the influent and effluent samples. The error bars represent one standard deviation from the mean value.

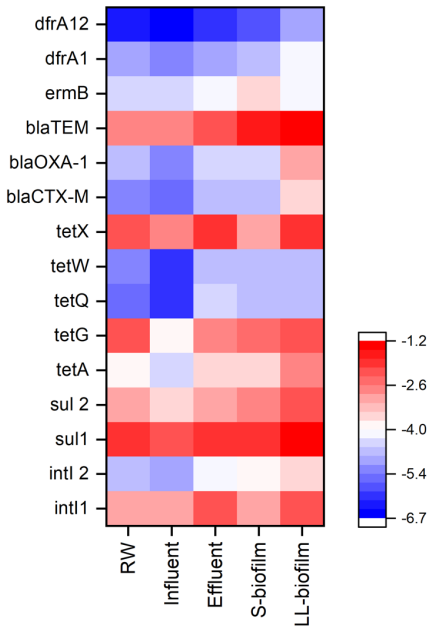

Figure 5 A heatmap showing the distinct patterns of the relative abundance (normalised to *16S rRNA*) of ARGs in raw water (RW), influent, effluent, S-biofilm (surface layer biofilm), and LL-biofilm (lower layer biofilm) samples.

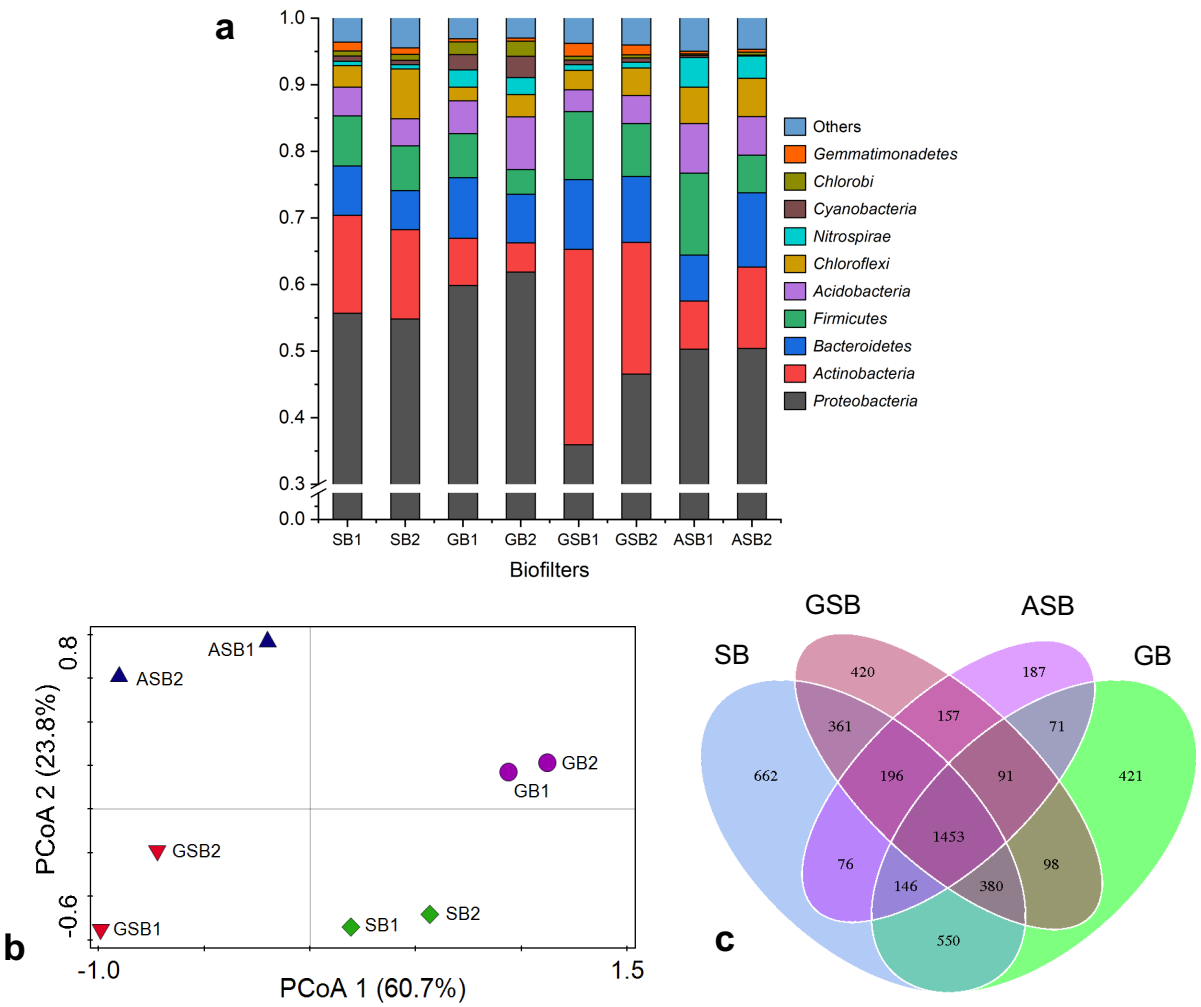

Figure 6 (a) Structure of surface layer biofilm microbial community at phylum level. (b) Principal coordinate analysis (PCoA) based on the Bray-Curtis distance showing the overall distribution of bacterial species in surface layer biofilms; (c) Venn diagram showing the number of OTUs that are unique and shared between surface layer biofilms. SB: sand biofilter, GB: GAC biofilter; GSB: GAC sandwich biofilter; and ASB: anthracite-sand biofilter.

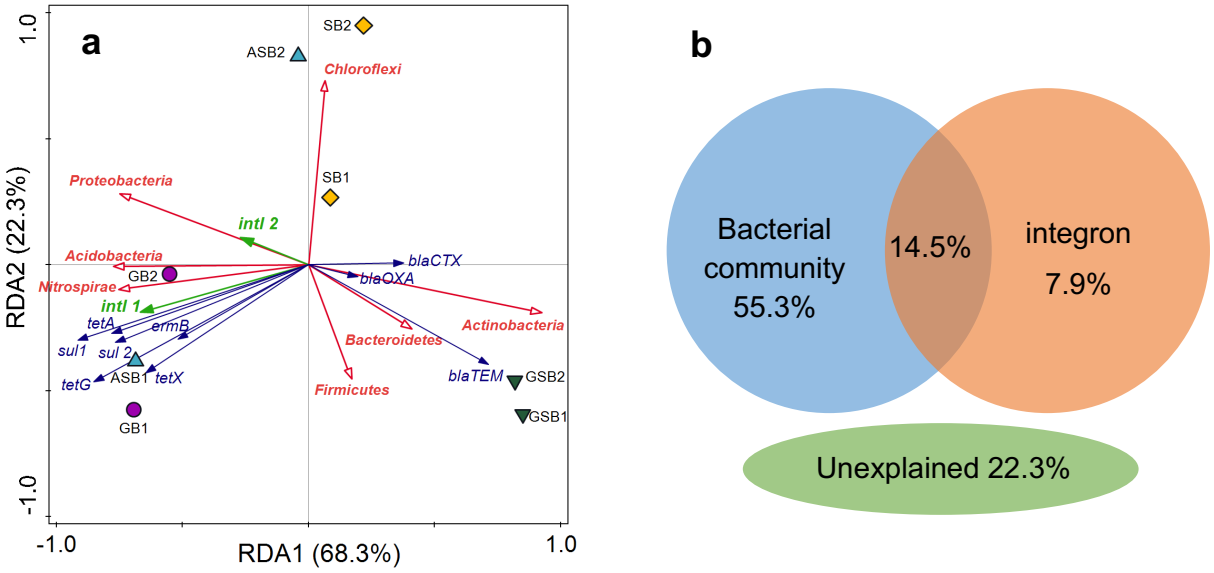

Figure 7 (a) Redundancy analysis (RDA) of the correlation between major phyla (1% in any samples) and target ARGs and integron genes in surface layer biofilm samples. The lengths of the arrows reveal the strength of the relationship and the angles between arrows indicate the correlation between specific genes and major phyla. (b) Variation partitioning analysis (VPA) differentiating effects of microbial community and integron on the ARGs variation in surface layer biofilm samples. *TetQ*, *tetW*, *dfrA1* and *dfrA12* were excluded from the analysis due to low detection frequency.

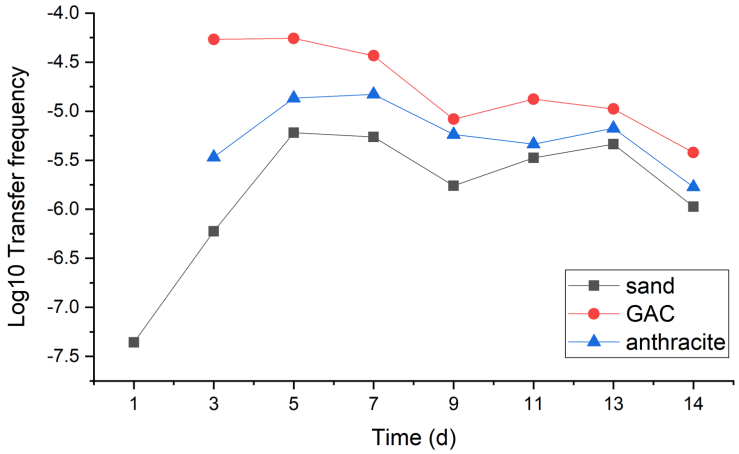

Figure 8 Dynamic changes of RP1 plasmid transfer frequency in media samples over time.

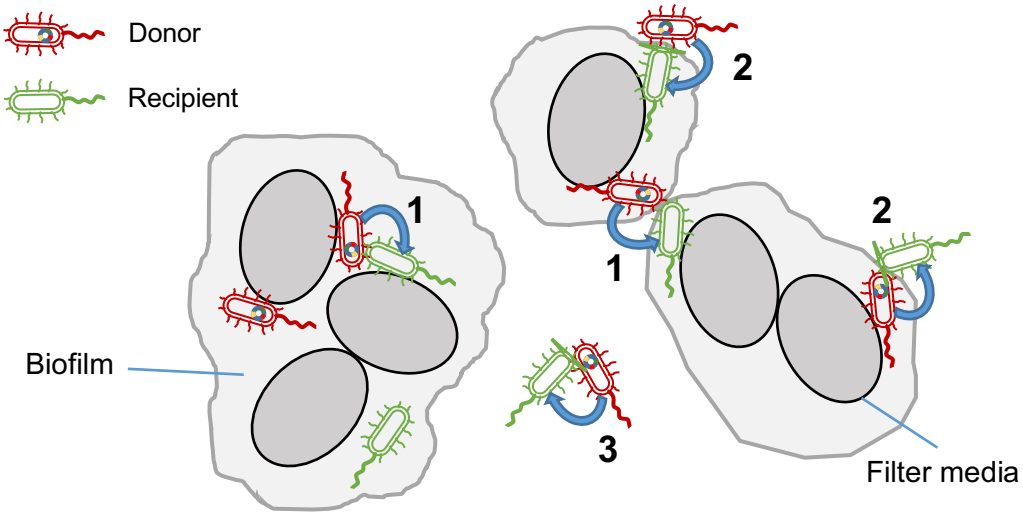

Figure 9 Conjugative transfer of RP1 plasmid within stationary phase (1); between stationary and planktonic phase (2); and in planktonic phase (3).

Supplementary Material

Drinking water biofiltration: behaviour of ARGs and the association with bacterial community

Like Xu, Luiza C. Campos, Melisa Canales, Lena Ciric *

Department of Civil, Environmental & Geomatic Engineering, University College London, London, WC1E 6BT, UK

* Corresponding author: Lena Ciric, l.ciric@ucl.ac.uk

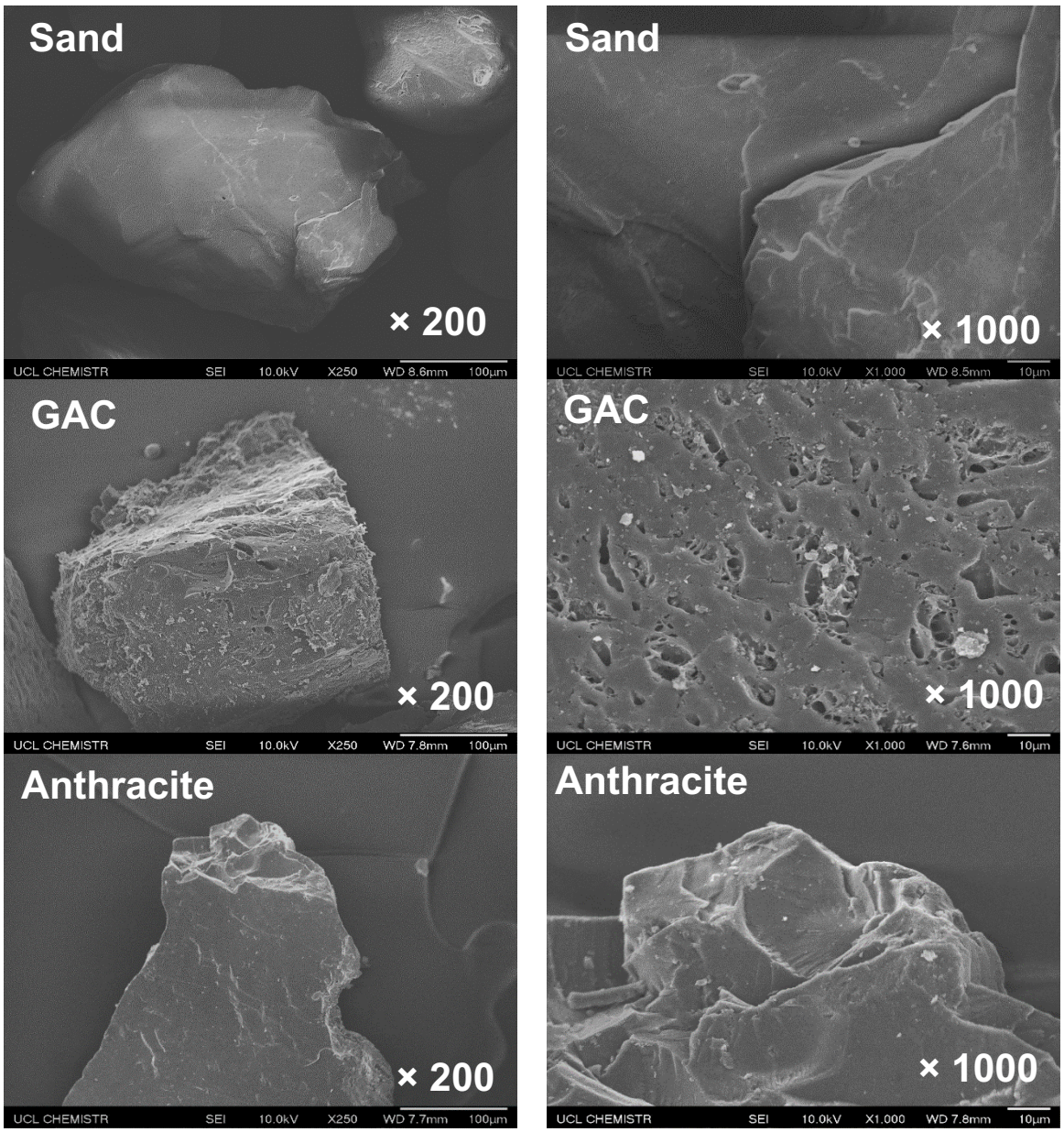

Figure S1 SEM (Scanning electron microscope) picture of the surface structure of sand, GAC and anthracite .

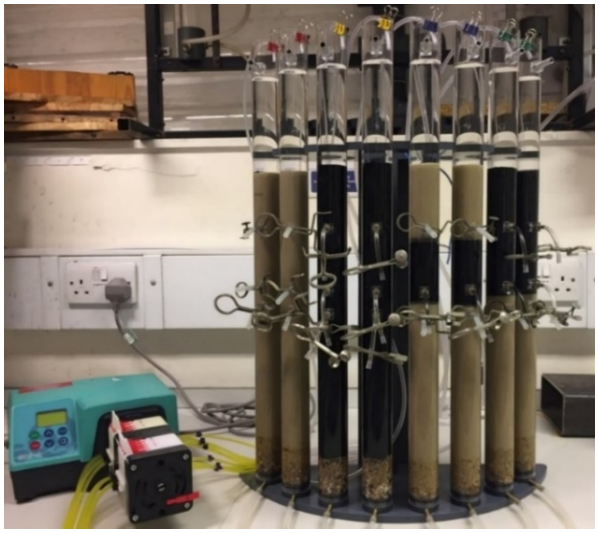

Figure S2 Schematic of biofilter column set-up. Sand, GAC, GAC sandwich, and anthracite-sand dual biofilters were set-up in duplicate (from left to right).

Determination of RP1 plasmid genotype

Based on the antibiotic resistance phenotype of the RP1 plasmid, two pairs of ARG primers, *bla*$_{TEM}$ and *tetA* were used to determine the antibiotic resistance genotype of the RP1 plasmid. Transconjugants were randomly selected from the plate and subjected to colony PCR to confirm the presence of the transferred plasmid. All the colony PCR assays were carried out using MutiGene Mini Thermal Cycler (Labnet International, UK). The reaction mixture consisted of 12.5 µL BioMixTM Red (BIOLINE, UK), 1 µL of each primer (10 µM), and 10.5 µL of PCR grade water. Individual colonies were picked using a sterile toothpick and dipped into each PCR reaction tube. Cycling conditions were as follows: 95 °C for 3 min, followed by 35 cycles at 95 °C for 15 s, 57 °C for 30 s, 75 °C for 30 s, and a final extension step at 72 °C for 7 min. Plasmid DNA carrying *bla*$_{CTX-M}$, *bla*$_{OXA-1}$, *bla*$_{TEM}$ and *tetA* were used as positive controls and PCR grade water was used as the negative control in every run. Six µL of the PCR products were verified by 1.5 % agarose gel electrophoresis and then visualised with a AlphaImager Mini System (Protein Simple, UK). All PCR products were sequenced by Source Bioscience (London, UK) and the results were compared with existing sequences using BLASTn alignment tool (https://blast.ncbi.nlm.nih.gov/Blast.cgi).

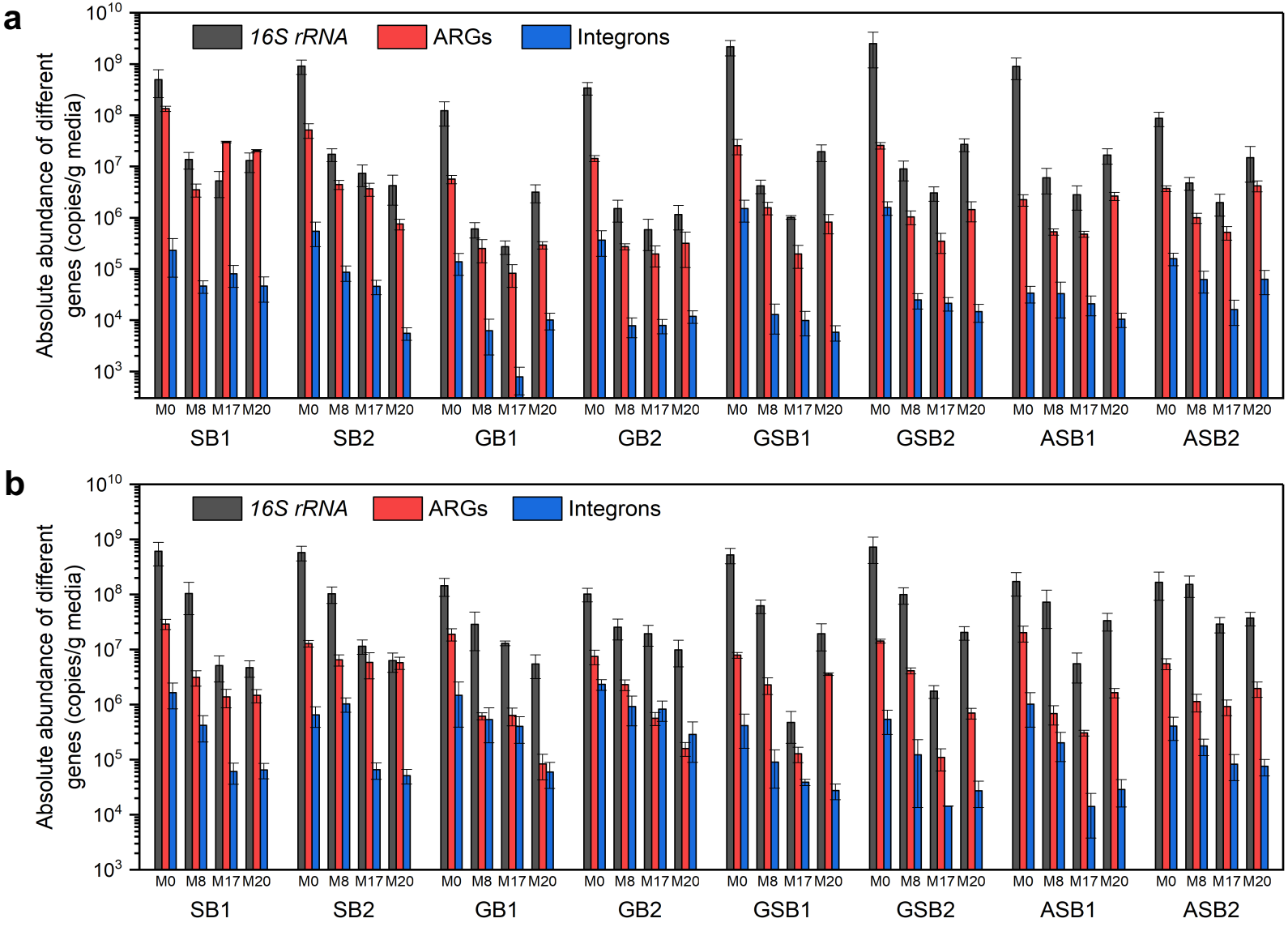

Figure S3 Absolute abundance of *16S rRNA* gene, ARGs and integrons (copies/g) in media samples at (a) 4-weeks and (b) 11-weeks of system run. Samples M0, M8, M17 and M20 refer to media (biofilm) samples collected at different sampling sites (0, 8, 17, and 20 cm). SB: sand biofilter; GB: GAC biofilter; GSB: GAC sandwich biofilter; ASB: anthracite-sand dual biofilter.

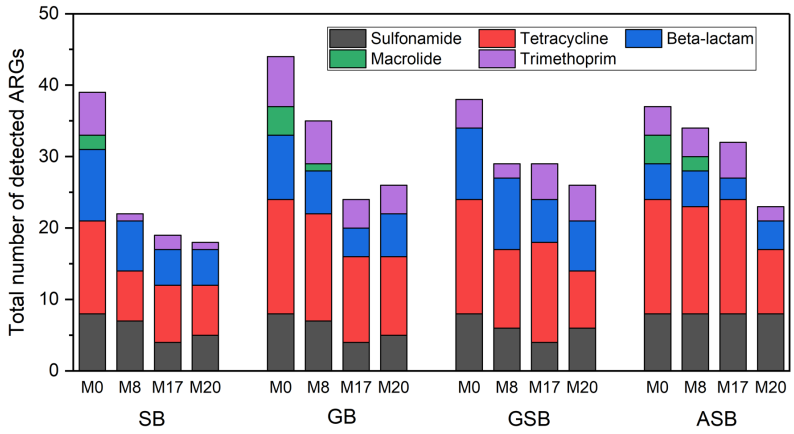

Figure S4 Richness of detected ARGs. Samples M0, M8, M17 and M20 refer to media (biofilm) samples collected at different sampling sites (0, 8, 17, and 20 cm). SB: sand biofilter; GB: GAC biofilter; GSB: GAC sandwich biofilter; ASB: anthracite-sand dual biofilter.

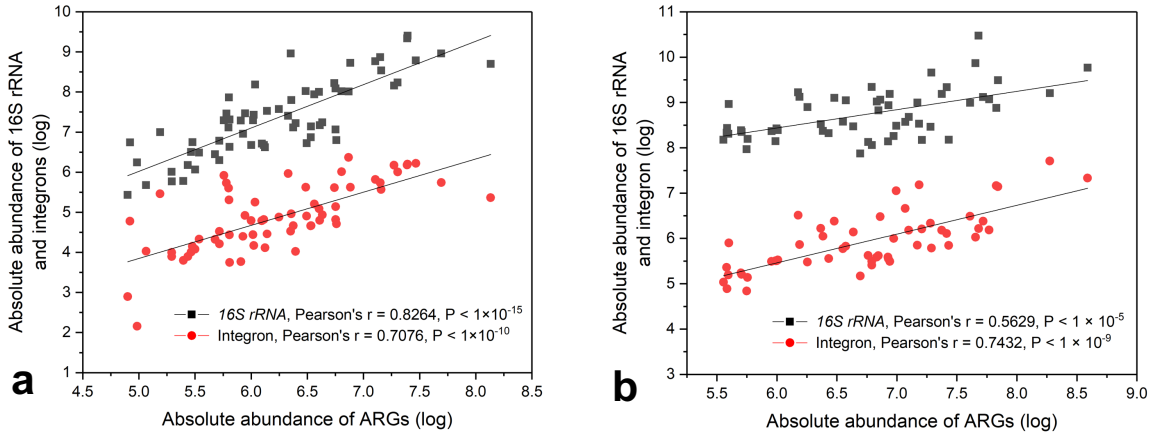

Figure S5 The correlations between the absolute abundance (log transformed) of ARGs and the corresponding *16S rRNA* gene and integrons in (a) biofilm samples; (b) influent and effluent samples.

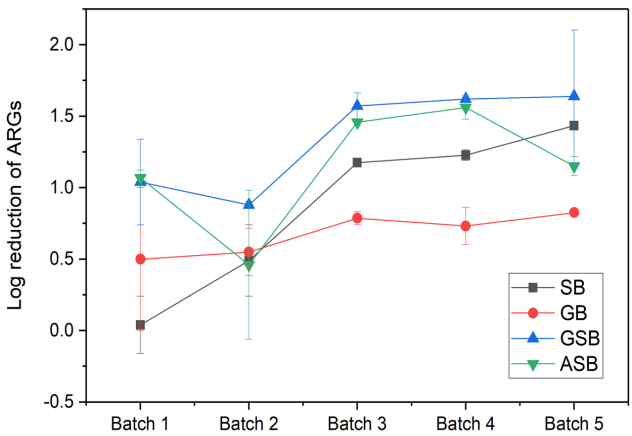

Figure S6 The reduction of ARGs (log transformed) in all biofilters. Batch 1: the week after the addition of antibiotics; Batch 2-4: every two weeks after batch 1; Batch 5: after the backwashing/ cleaning of the biofilters. SB: sand biofilter; GB: GAC biofilter; GSB: GAC sandwich biofilter; ASB: anthracite-sand biofilter.

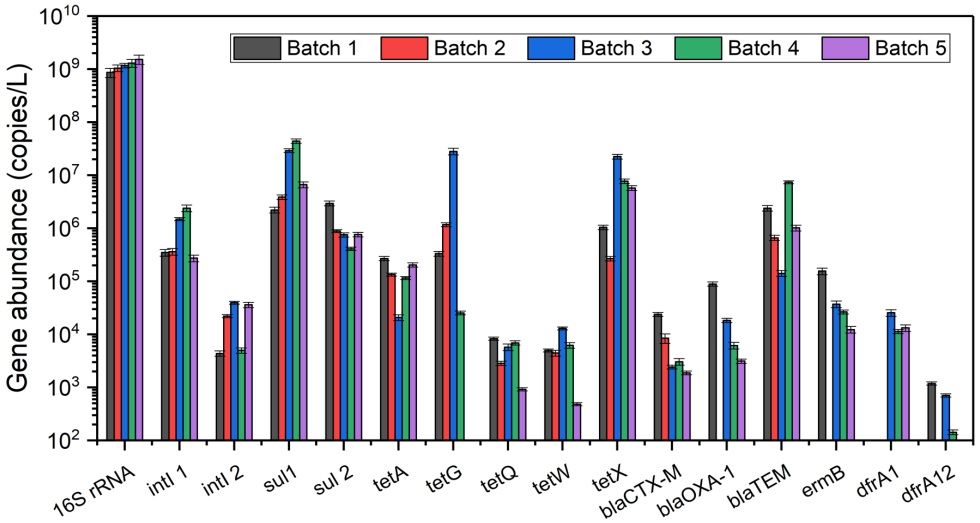

Figure S7 The concentration of the target genes in lake water samples.

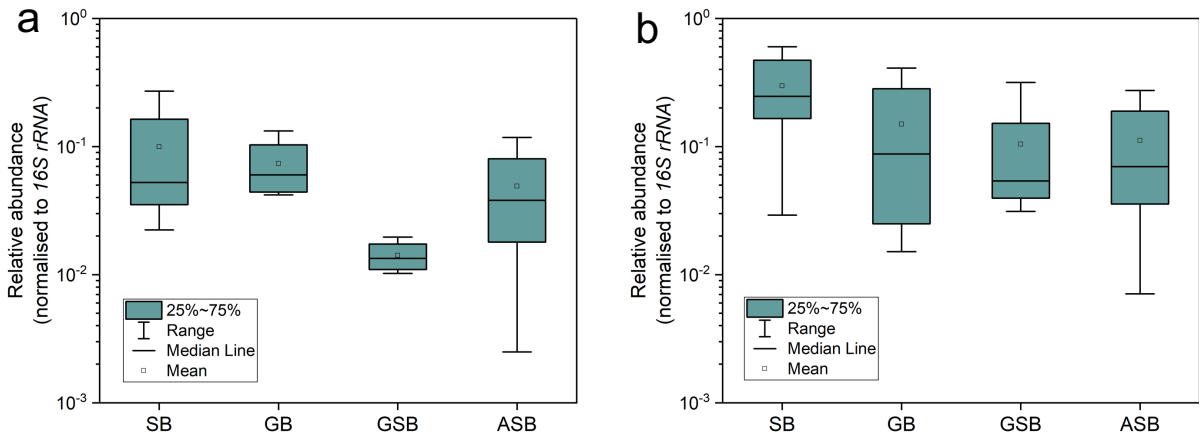

Figure S8 Relative abundance of ARGs (normalised to the *16S rRNA* gene) in (a) surface biofilms (M0); and (b) lower position biofilms (M8, M17 and M20) from different biofilters. SB: sand biofilter; GB: GAC biofilter; GSB: GAC sandwich biofilter; ASB: anthracite-sand dual biofilter.

Table S1 The correlation of the relative abundance of ARGs between raw water, influent, effluent, surface biofilm and lower layer biofilm samples in all biofilters.

Sample type	Surface biofilm	Lower layer biofilm	Raw water	Influent	Effluent
Surface biofilm	1				
Lower layer biofilm	0.895	1			
Raw water	0.524*	0.801	1		
Influent	0.614*	0.900	0.912	1	
Effluent	0.783	0.944	0.808	0.908	1

* $P < 0.05$; All other P values < 0.001.

Table S2 Correlation among ARGs in biofilm samples of each biofilter (n = 64) by Pearson correlation analysis.

	intI 1	*intI 2*	*sul1*	*sul2*	*tetA*	*tetG*	*tetQ*	*tetW*	*tetX*	bla_{CTX-M}	bla_{OXA-1}	bla_{TEM}	*ermB*	*dfrA1*	*dfrA12*	∑*int*	∑*sul*	∑*tet*	∑*bla*	∑*dfrA*	∑*ARGs*
intI 1	1.00																				
intI 2	**0.45***	1.00																			
sul1	**0.61****	**0.73****	1.00																		
sul2	**0.41****	**0.69****	**0.76****	1.00																	
tetA	**0.47****	**0.50****	**0.64****	**0.59****	1.00																
tetG	**0.41***	0.41	**0.82****	**0.72****	**0.74****	1.00															
tetQ	0.17	0.22	0.30	**0.53***	**0.84****	**0.75****	1.00														
tetW	0.22	0.23	**0.56****	**0.86****	**0.84****	**0.75****	**0.89****	1.00													
tetX	-0.06	0.24	0.04	**0.56****	**0.49****	**0.63****	**0.43***	0.05	1.00												
bla_{CTX-M}	0.14	**0.67****	**0.35****	**0.35***	**0.45****	0.04	**0.62****	**0.96****	-0.04	1.00											
bla_{OXA-1}	0.03	**0.88****	0.20	**0.63****	**0.41***	-0.06	**0.88***	**0.93***	0.08	0.19	1.00										
bla_{TEM}	-0.19	-0.04	0.12	0.44	**0.79****	**0.69****	**0.99****	**0.91****	**0.43***	0.11	0.07	1.00									
ermB	-0.19	-0.02	0.03	0.51	**0.83****	**0.66***	**1.00****	**1.00****	**0.93****	0.25	0.05	**1.00****	1.00								
dfrA1	-0.07	-0.03	0.22	**0.53***	**0.87****	**0.85****	**1.00****	**1.00****	0.06	0.25	0.13	**1.00****	**1.00****	1.00							
dfrA12	0.14	0.11	**0.37***	**0.47****	**0.82****	**0.66***	**0.98****	**0.93****	**0.39***	0.23	0.28	**0.96****	**0.93****	**0.99****	1.00						
∑*int*	**0.99****	**0.58****	**0.66****	**0.46****	**0.50****	**0.43***	0.18	0.22	-0.06	0.22	0.09	-0.18	-0.18	-0.06	0.15	1.00					
∑*sul*	**0.60****	**0.75****	**1.00****	**0.82****	**0.65****	**0.85****	0.35	**0.63****	0.03	**0.37****	0.19	0.18	0.10	0.27	**0.40****	**0.65****	1.00				
∑*tet*	**0.44****	0.06	**0.54****	**0.34***	**0.64****	**1.00****	**0.78****	**0.63****	**0.97****	0.07	0.00	**0.68****	**0.70****	**0.85****	**0.66****	**0.43****	**0.54****	1.00			
∑*bla*	0.06	0.07	**0.25***	**0.49****	**0.70****	**0.62****	**0.99****	**0.93****	0.01	0.25	0.05	**1.00****	**1.00****	**0.99****	**0.89****	0.07	**0.29***	**0.64****	1.00		
∑*dfrA*	0.00	0.03	0.14	**0.37***	**0.63****	**0.63****	**0.98****	**0.82****	0.11	0.19	0.03	**0.97****	**1.00****	**1.00****	**0.85****	0.01	0.18	**0.65****	**0.96****	1.00	
∑*ARGs*	**0.25***	0.25	**0.52****	**0.66****	**0.81****	**0.78****	**0.96****	**0.95****	**0.23***	**0.32***	0.09	**0.97****	**0.97****	**0.97****	**0.90****	**0.27***	**0.56****	**0.75****	**0.96****	**0.89****	1.00

Values indicate the Pearson correlation coefficient (r). The bold number means the significant level at the 0.05 level (2-tailed *) and 0.01 level (2-tailed **), otherwise means $p > 0.05$. ∑int: total concentration of integron genes (intI 1 and intI 2); ∑sul: total concentration of sulfonamide resistance genes (sul1 and sul2); ∑tet: total concentration of tetracycline resistance genes (tetA, tetG, tetQ, tetW); ∑bla: total concentration of β-lactams resistance genes; ∑dfrA: total concentration of resistance trimethoprim genes (dfrA1 and dfrA12). ∑ARGs: total concentration of all ARGs detected in this study.

Table S3 Correlation among ARGs in aqueous samples of each biofilter (n = 54) by Pearson correlation analysis.

	intI1	*intI 2*	*sul1*	*sul 2*	*tetA*	*tetG*	*tetQ*	*tetW*	*tetX*	bla_{CTX-M}	bla_{OXA-1}	bla_{TEM}	*ermB*	*dfrA1*	*dfrA12*	∑*int*	∑*sul*	∑*tet*	∑*bla*	∑*dfrA*	∑*ARGs*
intI1	1.00																				
intI 2	**0.80****	1.00																			
sul1	**0.50****	0.39	1.00																		
sul 2	**0.29***	0.25	0.28	1.00																	
tetA	**0.89****	**0.77****	**0.53****	0.28	1.00																
tetG	0.22	0.20	0.17	0.10	0.20	1.00															
tetQ	**0.86****	**0.77****	0.21	0.19	**0.93****	0.19	1.00														
tetW	**0.85****	**0.77****	0.26	0.18	**0.93****	0.22	**1.00****	1.00													
tetX	-0.08	**0.35***	-0.03	-0.03	-0.05	0.19	0.01	0.01	1.00												
bla_{CTX-M}	**0.91****	**0.83****	**0.52****	**0.31***	**0.98****	0.20	**0.94****	**0.93****	-0.03	1.00											
bla_{OXA-1}	0.24	0.15	0.23	**0.51****	0.06	0.08	-0.01	-0.04	-0.01	0.19	1.00										
bla_{TEM}	**0.91****	**0.87****	**0.47****	**0.38****	**0.93****	0.21	**0.91****	**0.90****	-0.01	**0.97****	0.28	1.00									
ermB	**0.57****	0.49	**0.51***	**0.81****	0.39	0.13	0.35	0.35	-0.21	**0.47***	**0.74****	**0.60****	1.00								
dfrA1	0.19	**0.55***	**0.43****	**0.36***	0.19	0.23	0.09	0.13	**0.31***	0.26	**0.50****	**0.31***	0.30	1.00							
dfrA12	**0.94****	**0.79****	**0.53****	**0.34***	**0.99****	0.24	**0.94****	**0.94****	-0.01	**0.99****	0.11	**0.97****	**0.72****	0.19	1.00						
∑*int*	**1.00****	**0.80****	**0.50****	**0.29***	**0.89****	0.22	**0.86****	**0.85****	-0.08	**0.91****	0.24	**0.91****	**0.57****	0.19	**0.94****	1.00					
∑*sul*	**0.50****	0.39	**1.00****	**0.30***	**0.53****	0.17	0.21	0.26	-0.03	**0.52****	0.24	**0.48****	**0.55****	**0.43****	**0.53****	**0.50****	1.00				
∑*tet*	**0.35***	0.31	0.24	0.16	**0.33***	**0.99****	**0.32***	**0.35***	**0.94****	**0.33***	0.11	**0.33***	0.19	0.26	**0.38****	**0.35****	0.24	1.00			
∑*bla*	**0.91****	**0.87****	**0.47****	**0.39****	**0.93****	0.21	**0.91****	**0.90****	0.00	**0.97****	**0.29***	**1.00****	**0.61****	**0.30***	**0.97****	**0.91****	**0.48****	**0.34***	1.00		
∑*dfrA*	0.26	**0.70****	**0.46****	0.21	**0.35***	0.24	0.28	**0.33***	**0.32***	**0.40****	0.13	**0.43****	-0.06	**0.98****	**0.36***	0.26	**0.46****	**0.29***	**0.43****	1.00	
∑*ARGs*	**0.75****	**0.64****	**0.94****	**0.37****	**0.76****	0.27	**0.52****	**0.55****	0.14	**0.77****	**0.29***	**0.74****	**0.62****	**0.43****	**0.77****	**0.75****	**0.94****	**0.37****	**0.74****	**0.50****	1.00

Values indicate the Pearson correlation coefficient (r). The bold number means the significant level at the 0.05 level (2-tailed *) and 0.01 level (2-tailed **), otherwise means p > 0.05. ∑int: total concentration of integron genes (intI 1 and intI 2); ∑sul: total concentration of sulfonamide resistance genes (sul1 and sul2); ∑tet: total concentration of tetracycline resistance genes (tetA, tetG, tetQ, tetW); ∑bla: total concentration of β-lactams resistance genes; ∑dfrA: total concentration of resistance trimethoprim genes (dfrA1 and dfrA12). ∑ARGs: total concentration of all ARGs detected in this study.

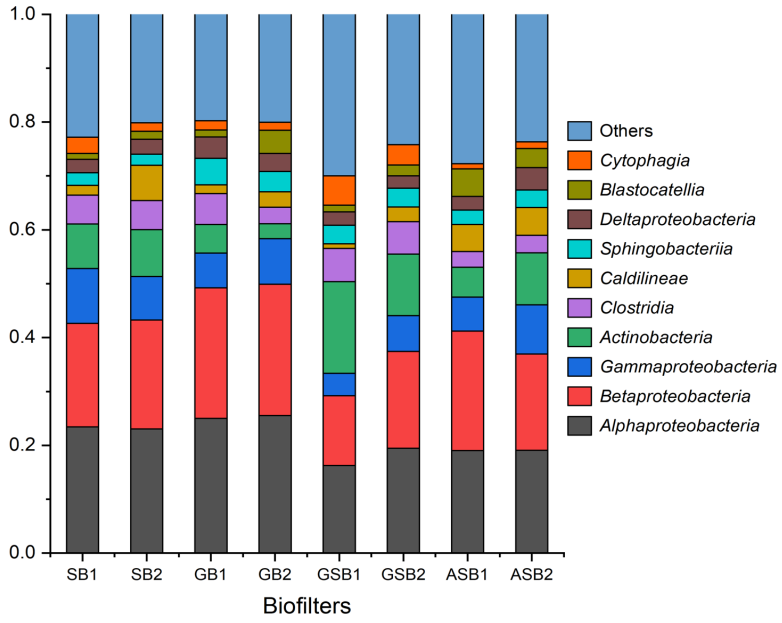

Figure S9 Structure of bacterial community (> 1% in any samples) at class level. SB: sand biofilter; GB: GAC biofilter; GSB: GAC sandwich biofilter; ASB: anthracite-sand dual biofilter.

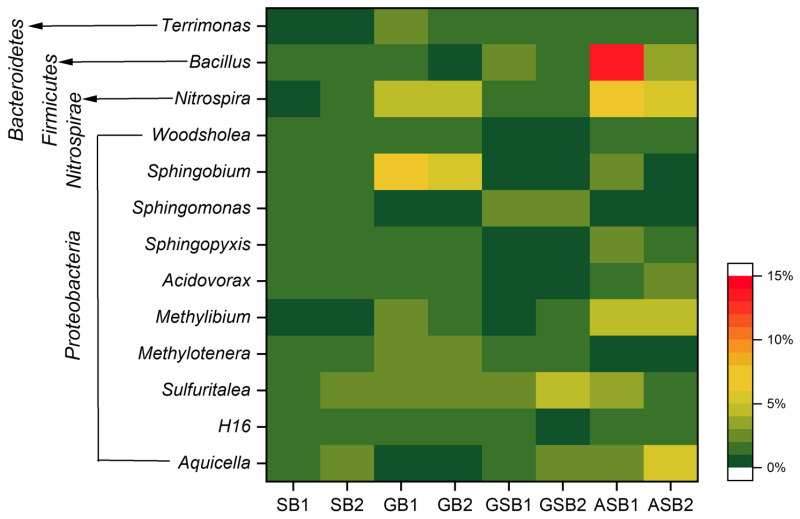

Figure S10 Relative abundance of each taxonomic genus (>1 % in any sample) in the surface biofilm samples of sand biofilter (SB), GB (GAC biofilter), GSB (GAC sandwich biofilter), and ASB (anthracite-sand biofilter) biofilm samples. The colour intensity in each panel shows the percentage of each genus in one sample.

Table S4 The percentage relative abundance of genera associated with opportunistic human pathogens.

Genera	SB1	SB2	GB1	GB2	GSB1	GSB2	ASB1	ASB2
Acinetobacter	1.280	0.258	0.033	0.035	0.161	0.154	0.066	0.069
Aeromonas	0.544	0.101	0.017	0.020	0.016	0.020	0.032	0.004
Bacillus	1.293	0.989	0.649	0.499	1.893	1.145	8.589	2.060
Clostridium	0.140	0.056	0.015	0.016	0.183	0.017	0.008	0.011
Escherichia	0.023	0.078	0.004	0.018	0.018	0.372	0.001	0.039
Legionella	1.009	0.795	0.369	0.311	0.081	0.134	0.239	0.252
Mycobacterium	0.255	0.301	0.477	0.554	0.199	0.358	0.845	1.288
Pseudomonas	0.079	0.075	0.095	0.076	0.409	0.547	2.003	1.138
Streptococcus	0.003	0.013	0.003	0.006	0.018	0.045	0.079	0.013

SB: sand biofilter; GB: GAC biofilter; GSB: GAC sandwich biofilter; ASB: anthracite-sand dual biofilter.

Table S5 Correlation between ARGs and major bacterial phyla in biofilm samples (n = 8) by Pearson correlation analysis.

ARGs	*Proteobacteria*	*Firmicutes*	*Actinobacteria*	*Acidobacteria*	*Bacteroidetes*	*Chloroflexi*	*Nitrospirae*
intI1	**0.65***	-0.52	**-0.68***	**0.75****	-0.27	-0.36	0.40
intI2	**0.63***	-0.41	-0.31	0.03	-0.48	-0.40	-0.34
sul1	0.55	0.15	**-0.76****	**0.60***	-0.31	-0.21	**0.74****
sul2	**0.75****	-0.39	**-0.70***	0.42	-0.24	-0.52	0.33
tetA	0.35	0.44	**-0.65***	**0.63***	-0.50	0.04	**0.72****
tetG	0.43	0.17	**-0.70***	**0.68***	-0.22	-0.25	**0.78****
tetX	0.54	-0.32	-0.54	0.33	0.01	-0.55	0.36
bla_{CTX-M}	-0.09	0.12	0.36	-0.45	-0.09	-0.29	-0.59
bla_{OXA-1}	0.07	0.04	0.21	-0.42	-0.07	-0.42	-0.51
bla_{TEM}	-0.46	0.21	**0.69***	-0.60	0.31	-0.47	**-0.68***
ermB	0.41	-0.14	-0.38	-0.01	0.17	-0.46	0.28
dfrA12	0.01	0.57	-0.43	0.60	-0.24	0.34	**0.82****

Values indicate the Pearson correlation coefficient (r). The bold number means the significant level at the 0.05 level (2-tailed *) and 0.01 level (2-tailed **), otherwise means P > 0.05. *TetQ*, *tetW* and *dfrA1* were excluded from the analysis due to low detection frequency.

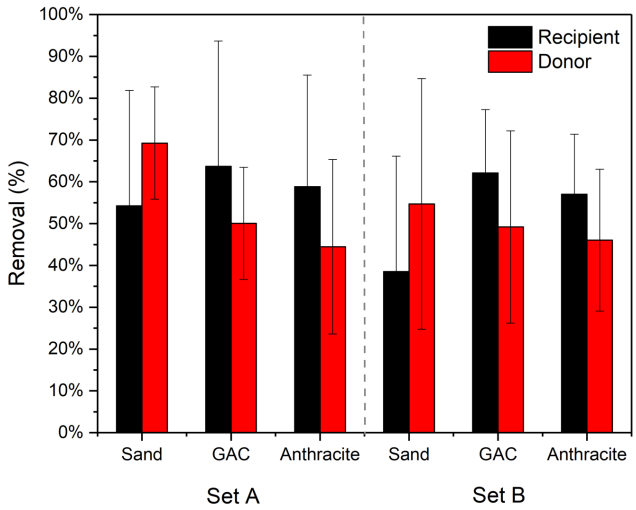

Figure S11 The removal of donor and recipient by biofilters. Set A: biofilters exposed to 2 μg/L of antibiotic mixture: Set B: biofilters without antibiotics exposure. The error bars represent STD from the mean value of all batch samples (n = 8).

79

80

81 **Table S6** The transfer frequency of RP1 plasmid (on average) in the influent and effluent of each
82 biofilters.

Time (d)	Influent		Effluent - Set A			Effluent – Set B		
	Set A	Set B	Sand	GAC	Anthracite	Sand	GAC	Anthracite
1	**3.42×10^{-7}**	n.a.	n.a.	n.a.	n.a.	n.a.	**2.40×10^{-6}**	n.a.
3	n.a.	n.a.	n.a.	n.a.	n.a.	n.a.	n.a.	**4.48×10^{-5}**
5	**4.93×10^{-6}**	n.a.	n.a.	**1.56×10^{-5}**	n.a.	n.a.	n.a.	n.a.
7	n.a.	n.a.	n.a.	n.a.	**1.72×10^{-5}**	n.a.	n.a.	**6.58×10^{-6}**
9	n.a.	n.a.	n.a.	n.a.	**2.16×10^{-5}**	n.a.	n.a.	n.a.
11	**3.36×10^{-6}**	**3.25×10^{-6}**	n.a.	n.a.	n.a.	n.a.	n.a.	n.a.
13	**3.72×10^{-6}**	n.a.	n.a.	n.a.	n.a.	n.a.	**1.47×10^{-5}**	n.a.
***14**	**1.90×10^{-5}**	**1.92×10^{-5}**	**1.60×10^{-5}**	**4.55×10^{-5}**	**3.07×10^{-5}**	n.a.	n.a.	**1.66×10^{-5}**

83 Set A: biofilters exposed to 2 μg/L of antibiotic mixture: Set B: biofilters without antibiotics exposure.
84 *14: backwash was conducted for the system.

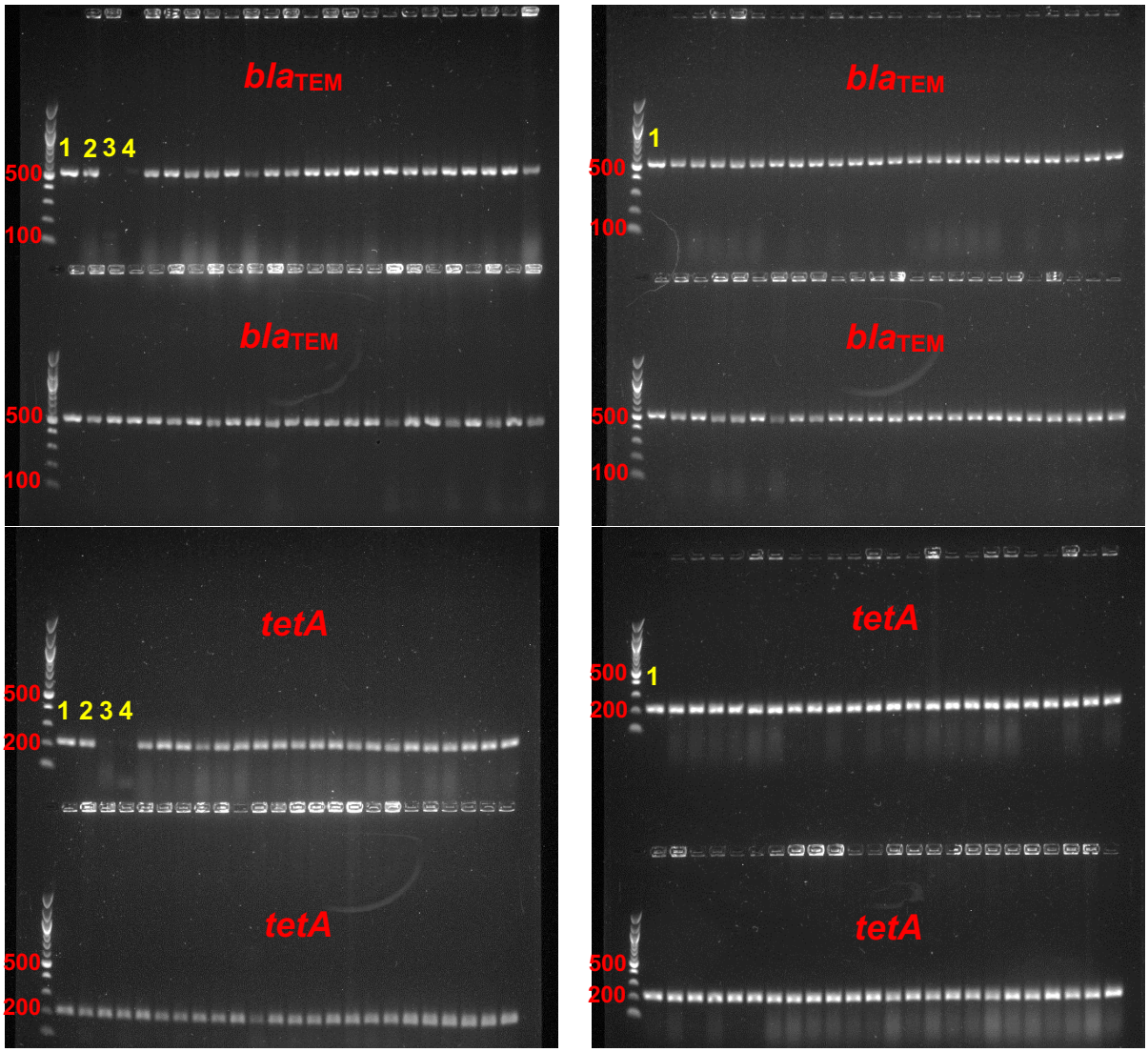

Figure S12 Gel images showed the presence of *bla*$_{TEM}$ (516 bp) and *tetA* (210 bp) in all of the transconjugants. Lane 1: RP1 plasmid as positive control; Lane 2: donor cell (*E. coli* J53); Lane 3: recipient cell (*E. coli* HB101); Lane 4: PCR negative control. The rest of the lanes are colonies randomly selected from the plates on which transconjugants grew.